ADDIS ABABA UNIVERSITY

FACULTY OF TECHNOLOGY

DEPARTMENT OF MECHANICAL ENGINEERING

SCHOOL OF GRADUATE STUDIES

MECHANICAL DESIGN STREAM

Design and Analysis of a Mechanical Damper in a Milling Cutter

By: **Tassew Girma**

Advisor: **Dr.-Ing. Tamrat Tesfaye**

A THESIS SUBMITTED IN PARTIAL FULFILLMENT OF THE REQUIREMENTS OF THE MASTER'S OF SCIENCE DEGREE IN MECHANICAL ENGINEERING.

July 2009

I, the undersigned, declare that this thesis work is my original work and has not been presented for a degree in any other university, and that all sources of material are duly acknowledged.

Name: - **Tassew Girma Mengistu**

Place: - **Addis Ababa University**

Date of Submission: - _____

Signature: - _____

Title of the thesis:-

Design and Analysis of a Mechanical Damper in Milling Cutter

This thesis has been presented for the evaluation with my approval as a university advisor.

Dr.-Ing. Tamrat Tesfaye _____ _____

Table of Contents

Acknowledgments

I would like to express my deepest gratitude to my advisor Dr.-Ing Tamrat Tesfaye for his inspiration, support and guidance during this research. Special thanks go to Ato Kibret Alemayehu for his help in completing tasks associated with the research. My appreciation also goes to Ato Desalegn Damena for his endless efforts in giving me morale and support. Finally I wish to thank my family, especially my brother Wegayehu Girma. Without their support and caring this work would not have been possible.

Abstract

When an endmill is used in high-speed machining, chatter vibration of the tool can cause undesirable results. This vibration increases tool wear and leaves chatter marks on the cutting surface. To reduce the chatter vibration, a layered-beam damper is inserted into the hole at the center of the tool. The friction work done by the relative motion between the tool and damper reduces chatter vibration. The purpose of this research is to design and optimize the configuration of the damper to obtain the maximum damping effect.

The analytical method has been reviewed, which is based on the assumption of constant contact pressure and uniform deflection. For the numerical approach, nonlinear finite element analysis is employed to calculate the distribution of the contact pressure under the centrifugal and cutting forces. The analytical and numerical results are compared and discussed.

In order to identify the effect of the damper's configuration, two design variables are chosen: the inner radius of the damper and the number of slotted dampers. During the parameter study and optimization, the inner radius is varied from 1.5mm to 3.5mm and the number of slotted dampers is varied from 2 to 10.

Results show that the damping effect is maximum when the inner radius is 1.5mm and the number of slotted dampers is 5. However, this result depends on the operating condition. Thus, it is suggested to prepare a set of dampers and to apply the appropriate one for the optimum damping effect for a given operating condition.

Chapter 1

Introduction

1.1 Background

The availability of various machine tools, even the most up-to-date ones, in sufficient quantities does not itself ensure efficient and highly productive operation of an industrial enterprise without appropriate organization and proper use of its equipment.

Proper use of machine tools is aimed at obtaining the maximum productive output and accuracy over a long period of service. The maximum productive output is obtained by correct selection of cutting tools and cutting speeds and feeds, and also by proper setting-up and adjustment of the machine tool.

Proper use of machine tools involves appropriate packing, transportation, shop installation, servicing, certification, repair, and modernization. Proper packing and transportation prevent damage of machine tools. Correct installation of machine tools helps to insure trouble-free operation. Tests of machine tools are necessary for checking their static and dynamic accuracy, power consumption, rigidity, vibration-proof properties, etc.

Milling is widely used in many areas of manufacturing. Traditionally, milling has been regarded as a slow and costly process. Therefore many efforts have been made to improve the efficiency of milling .The main limitation of milling is caused by the vibration of the machine tool and workpiece .As the speed and the power of milling are increased, it is very important to control vibration of the tool.

Two different kinds of vibration affect the cutting operation. The one is the self-excited (chatter) vibration at the high spindle speed, and the other is vibration at the

critical natural frequency. This research is focused on the former, which produces a wavy surface during the milling operation.

1.2 Motivation of the Thesis

What motivated me to work this research are:

-The booming industries in our country and the demand of quality products.

-Curiosity to design a mechanical part that solves problems in machining.

-The desire to ensure efficient and highly productive industrial sectors.

-The newly emerging investments in our country and their demand of sophisticated machines and equipment.

1.3 Objective of the Thesis

1.3.1 General Objective of the Thesis

The general objective of the thesis is to improve the productivity of the manufacturing sector thereby increasing the quality of products.

1.3.2 Specific Objectives

The other objectives of the the thesis are:

-To design a damper of optimum configuration;

-To create easy working condition for the person working on the milling machine.

-To assess the vibration problem and the existing damping mechanism.

-To avoid chatter marks on the cutting surface.

-To calculate the amount of friction work and to maximize its effect by changing the damper's configuration.

1.4 Scope of the Thesis

The scope of this thesis is mentioned hereunder:

-The forces that have been considered are vertical and centrifugal forces.

1.5 Thesis Approach

The organization of this thesis is as follows.

Chapter 2 presents a literature review in which literatures gathered from different books and the internet are included.

In **chapter 3**, a simplified model of the endmill is introduced that can be used for analytical study and numerical simulation.

In **chapter 4**, the analytical approach is reviewed that qualitatively estimates the damping work. Here the calculation of frictional work and how it is derived from the beginning are presented step by step.

Chapter 5 describes the numerical simulation procedure using the finite element method. A simplified geometry of end-mill in chapter 3 is used here for finite element analysis.

Chapter 6 represents the result analysis by variation of parameters according to the change of two design variables which are the inner radius of the damper (finger) and the number of the damper (finger).

Chapter 7 talks about conclusions, recommendations and future work of the research.

Chapter 2

Literature Review

Milling cutters are cutting tools used in milling machines or machining centre. They remove material by their movement within the machine (e.g.: a ball nose mill) or directly from the cutters shape (a form tool such as a Hobbing cutter).

2.1 Features of a milling cutter

Milling cutters come in several shapes and many sizes. There is also a choice of coatings, as well as rake angle and number of cutting surfaces.

Shape: Several standard shapes of milling cutter are used in industry today, which are explained in more detail below.

Flutes / teeth: The flutes of the milling bit are the deep helical grooves running up the cutter, while the sharp blade along the edge of the flute is known as the tooth. The tooth cuts the material, and chips of this material are pulled up the flute by the rotation of the cutter. There is almost always one tooth per flute, but some cutters have two teeth per flute. Often, the words *flute* and *tooth* are used interchangeably. Milling cutters may have from one to many teeth, with 2, 3 and 4 being most common. Typically, the more teeth a cutter has, the more rapidly it can remove material. So, a 4-tooth cutter can remove material at twice the rate of a 2-tooth cutter.

Helix angle: The flutes of a milling cutter are almost always helical. If the flutes were straight, the whole tooth would impact the material at once, causing vibration and reducing accuracy and surface quality. Setting the flutes at an angle allows the tooth to enter the material gradually, reducing vibration. Typically, finishing cutters have a higher rake angle (tighter helix) to give a better finish.

Center cutting: Some milling cutters can drill straight down (plunge) through the material, while others cannot. This is because the teeth of some cutters do not go all the way to the centre of the end face. However, these cutters can cut downwards at an angle of 45 degrees or so.

Roughing or Finishing: Different types of cutter are available for cutting away large amounts of material, leaving a poor surface finish (roughing), or removing a smaller amount of material, but leaving a good surface finish (finishing). A roughing cutter may have serrated teeth for breaking the chips of material into smaller pieces. These teeth leave a rough surface behind. A finishing cutter may have large number (4 or more) teeth for removing material carefully. However, the large number of flutes leaves little room for efficient swarf removal, so they are less good for removing large amounts of material.

Coatings: The right tool coatings can have a great influence on the cutting process by increasing cutting speed and tool life, and improving the surface

finish. Polycrystalline Diamond (PCD) is an exceptionally hard coating used on cutters which must withstand high abrasive wear. A PCD coated tool may last up to 100 times longer than an uncoated tool. However the coating cannot be used at temperatures above 600 degrees C, or on ferrous metals. Tools for machining aluminium are sometimes given a coating of TiAlN. Aluminium is a relatively sticky metal, and can weld itself to the teeth of tools, causing them to appear blunt. However it tends not to stick to TiAlN, allowing the tool to be used for much longer in aluminium.

Shank: The shank is the cylindrical (non-fluted) part of the tool which is used to hold and locate it in the tool holder. A shank may be perfectly round, and held by friction, or it may have a Weldon Flat, where a grub screw makes contact for increased torque without the tool slipping. The diameter may be different from the diameter of the cutting part of the tool, so that it can be held by a standard tool holder.

2.2 Types of milling cutter

End mill

Slot, end mill, and ballnose cutter

End mills (middle row in image) are those tools which have cutting teeth at one end, as well as on the sides. The words *end mill* is generally used to refer to flat bottomed cutters, but also include rounded cutters (referred to as *ball nosed*) and radiused cutters (referred to as *bull nose*, or *torus*). They are usually made from high speed steel (HSS) or carbide, and have one or more flutes. They are the most common tool used in a vertical mill.

Slot drill

Slot drills (top row in image) are generally two (occasionally three or four) fluted cutters that are designed to drill straight down into the material. This is possible because there is at least one tooth at the centre of the end face. They are so named for their use in cutting keyway slots. The words *slot drill* are usually assumed to mean a two fluted, flat bottomed end mill if no other information is given. Two fluted end mills are usually slot drills, three fluted sometimes are not, and four fluted usually are not

Roughing end mill

Roughing end mills quickly remove large amounts of material. This kind of end mill utilizes a wavy tooth form cut on the periphery. These wavy teeth form many successive cutting edges producing many small chips, resulting in a relatively rough surface finish. During cutting, multiple teeth are in contact with the workpiece reducing chatter and vibration. Rapid stock removal with heavy

milling cuts is sometimes called *hogging*. Roughing end mills are also sometimes known as ripping cutters.

Ball nose cutter

Ball nose cutters (lower row in image) are similar to slot drills, but the ends of the cutters are hemispherical. They are ideal for machining 3-dimensional contoured shapes in machining centres, for example in moulds and dies. They are sometimes called *ball mills* in shop-floor slang, despite the fact that that term also has another meaning. They are also used to add a radius between perpendicular faces to reduce stress concentrations.

Slab mill

HSS slab mill

Slab mills are used either by themselves or in gang milling operations on manual horizontal or universal milling machines to machine large broad surfaces quickly. They have been superseded by the use of Carbide tipped face mills which are then used in vertical mills or machining centers.

Side-and-face cutter

Side and face cutter

The side-and-face cutter is designed with cutting teeth on its side as well as its circumference. They are made in varying diameters and widths depending on the application. The teeth on the side allow the cutter to make *unbalanced cuts* (cutting on one side only) without deflecting the cutter as would happen with a slitting saw or slot cutter (no side teeth).

Involute gear cutter

Involute gear cutter - No. 4

The image shows a *Number 4* cutter from an involute gear cutting set. There are 8 cutters (excluding the rare half sizes) that will cut gears from 12 teeth through to a rack (infinite diameter). The cutter shown has markings that show it is a 10 DP

(diametrical pitch) cutter. That it is No. 4 in the set that it cuts gears from 26 through to 34 teeth. It will cut gears with teeth giving the gear a 14.5 degree pressure angle

Hobbing cutter

These cutters are a type of form tool and are used in hobbing machines to generate gears. A cross section of the cutters tooth will generate the required shape on the workpiece, once set to the appropriate conditions (blank size). A hobbing machine is a specialised milling machine.

Face mill (indexable carbide insert)

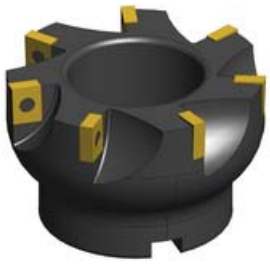

A face mill consists of a cutter body (with the appropriate machine taper) that is designed to hold multiple disposable carbide or ceramic tips or inserts, often golden in color. The tips are not designed to be resharpened and are selected from a range of types that may be determined by various criteria, some of which may be: tip shape, cutting action required, and material being cut. When the tips

are blunt, they may be removed, rotated (indexed) and replaced to present a fresh, sharp face to the workpiece, this increases the life of the tip and thus their economical cutting life.

Fly cutter

A fly cutter is composed of a body into which one or two tool bits are inserted. As the entire unit rotates, the tool bits take broad, shallow facing cuts. Fly cutters are analogous to face mills in that their purpose is face milling and their individual cutters are replaceable. Face mills are more ideal in various respects (e.g., rigidity, indexability of inserts without disturbing effective cutter diameter or tool length offset, depth-of-cut capability), but tend to be expensive, whereas fly cutters are very inexpensive.

Woodruff cutter

Various sizes of woodruff key cutters and keys

Woodruff cutters make the seat for woodruff keys. These keys locate pulleys on shafts and are shaped as shown in the image.

Hollow mill

Hollow milling cutters, more often called simply *hollow mills*, are essentially "inside-out endmills". They are shaped like a piece of pipe (but with thicker walls), with their cutting edges on the inside surface. They are used on turret lathes and screw machines as an alternative to turning with a box tool, or on milling machines or drill presses to finish a cylindrical boss (such as a trunnion).

2.3 Selecting a milling cutter

Selecting a milling cutter is not a simple task. There are many variables, opinions and lore to consider, but essentially the machinist is trying to choose a tool which will cut the material to the required specification for the least cost. The cost of the job is a combination of the price of the tool, the time taken by the milling machine, and the time taken by the machinist. Often, for job of a large number of parts, and days of machining time, the cost of the tool is lowest of the three costs.

- **Material:** High speed steel (HSS) cutters are the least-expensive and shortest-lived cutters. Cobalt steel is an improvement on HSS and generally can be run 10% faster. Carbide tools are more expensive than steel, but last longer, and can be run much faster, so prove more economical in the long run. HSS tools are perfectly adequate for many applications. The progression from HSS to cobalt steel to carbide could be viewed as very good, even better, and the best.

- **Diameter:** Larger tools can remove material faster than small ones, therefore the largest possible cutter that will fit in the job is usually chosen. When milling an internal contour, or concave external contours, the diameter is limited by the size of internal curves. The radius of the cutter must be less than or equal to the radius of the smallest arc.
- **Flutes:** More flutes allow a higher feed rate, because there is less material removed per flute. But because the core diameter increases, there is less room for swarf, so a balance must be chosen.
- **Coating:** Coatings, such as titanium nitrate, also increase initial cost but reduce wear and increase tool life.
- **Helix angle:** High helix angles are typically best for small metals, and low helix angles for hard or rough metals.

2.4 Vibration and Damper in Milling Cutter

Since machine members are elastic and frequently subjected to the action of vibratory forces, knowledge of the mechanics of vibration will assist the designer in reducing to a low value the deflections which these forces are likely to produce. The various types of a machine tend to vibrate at a frequency which is a function of the stiffness and the mass of the member. If the machine forces occur at a frequency which is near the natural vibration frequency of the member, then forces will be set up which may cause serious difficulties in the operation of the

machine and which will ultimately destroy it. Therefore, when vibratory forces are present, the designer should strive to design the members of the machine so that their natural frequencies are far removed from the frequencies of the forces.[1]

Various methods of preventing chatter have been incorporated into machine tool systems. In 1989, Cobb developed dampers for boring bar .These dampers are composed of two different types. The first type, which Cobb calls a shear damper, has two end "caps" that fit snugly around a boring bar. Between these are sandwiched an annular mass with plastic at each end, either in the form of ring or of several blocks at each end. This middle section of mass and plastic pieces has a clearance from the boring bar, and is preloaded between the end caps with bolts. When the boring bar vibrates, the end caps transmit this vibration through the plastic pieces to the annular mass, which vibrates in tune. Since the plastic pieces do not slide on the faces of either one, a shear force is produced on the end faces of the plastic. The viscoelastic properties of the plastic provide damping for the system. The other type of damper proposed by Cobb is the compression damper in which the mass is again an annulus. This annulus is cut in half down its axis to form two half annuli. These are then bolted together around rings of plastic that are in contact with the boring bar. The bolts provide a preload on the plastic rings, and when the bar vibrates, the annular mass vibrates out of phase with it, compressing one side and then the other of the plastic rings .This alternate squeezing of the plastic creates damping, again by deforming the plastic, but in a compressive rather than shearing manner.

In 1998, Dean focused on increasing the depth of cut and increasing axis federates to improve the metal removal rate (MRR). While he does not present any original ideas on

chatter reduction, his thesis refers to work done by Smith in which a chatter recognition system was developed. This system uses a microphone to detect the frequency of chatter when it occurs. The system then selects a different speed (according to the parameters of the system) and tries to machine again. This process repeats itself until chatter no longer occurs.

Much work in the field of structural damping has been done by Slocum. In order to damp vibrations, Slocum uses layered beams with viscoelastic materials between the layers. Two cantilevered beams are stacked on top of each other, and a force is applied to the end of the top beam. It is known that beams experience an axial shear force when displaced in this manner. Slocum's derivation calculates a relative displacement between corresponding points on the un-deformed beams. This is incorporated into a self damping structure by placing several small beams inside of a larger beam and injecting a viscoelastic material between them. This material bonds to each surface and thus, when there is a relative displacement, is deformed. The stretching of this material causes a dissipation of vibration energy and thus, damping.

In 2001, Sterling explored the possibility of deploying a damper directly inside of a rotating tool. To reduce the chatter vibration, a layered-beam, which Sterling calls a finger, is inserted into the hole at the center of the tool. Due to the high speed rotation, the outer surface of the damper contacts with the inner surface of the tool. When chatter vibration occurs, which is a deflection of the tool, work is done in the contact interface due to the friction force and the relative motion. This work is dissipative and reduces chatter vibration. He developed an analytical model and performed an experiment for the layered beam damper.

In this research, the work done by Sterling is further extended. Using finite element analysis, his analytical approach is compared to the numerical results. The objective of this research is to calculate the amount of friction work and to maximize its effect by changing the damper's configuration.

Chapter 3

Simplified Model

The machine tool that we are considering in this research is a 4 inch long endmill, as shown in Fig 3-1(a). Most endmills are of the solid beam type as shown in Fig 3-1a. In this type of tool, the only available damping mechanism is structural damping, which is very small. Structural damping, which is a variant of viscous damping, is usually caused by internal material friction. When the damping coefficient is small, as in the case of structures, damping is primarily effective at frequencies close to the resonant frequency of the structure.

When a layered-beam damper is inserted into the hollow tool (see the simplified model in Fig.3-1(b)), the high speed rotation causes a strong contact between the beam and tool. When chatter vibration occurs, it generates a relative motion between the beam and tool. Due to the contact force, this relative motion causes a friction force in the interface, which damps the vibration. In this research, this damping mechanism will be referred to as a mechanical damper.

While the tool geometry is very important for cutting performance, the objective of this research is on the vibration of the tool. Thus, we want to simplify the tool geometry so that the analytical and numerical studies in the following chapters will be convenient.

The first step of simplifying the endmill model is to suppress unnecessary geometric details, while maintaining the endmill's mechanical properties. The endmill model can be simplified as a cylinder because we are only interested in the contact surface, which is the inner surface of the tool. Fig 3-1b illustrates the simplified model.

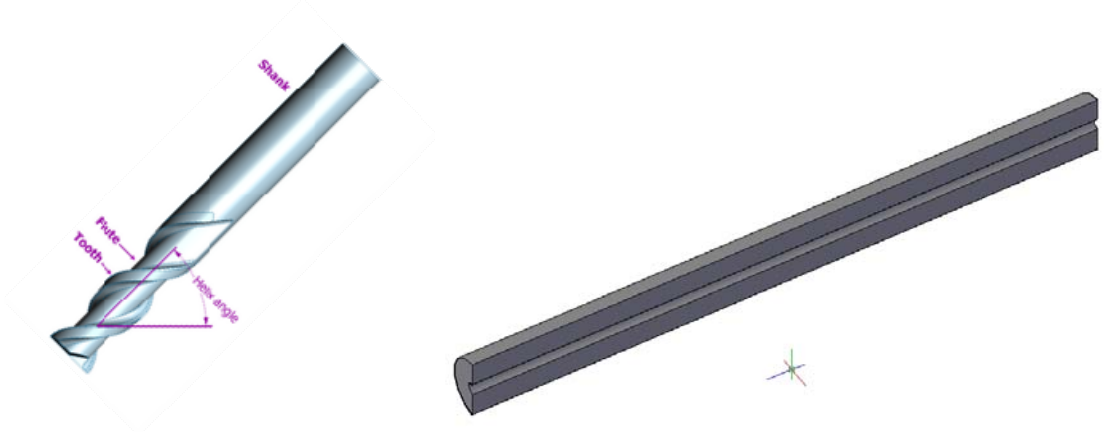

(a) The original solid endmill (b) A damper (Finger)

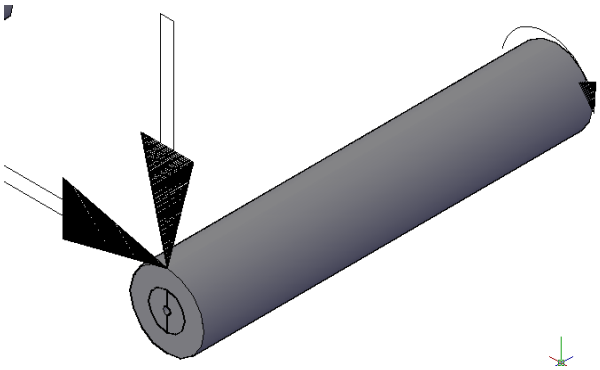

(b) The simplified endmill model using hollowed cylinders.

Figure 3.1. Endmill and model simplification.

The simplified endmill model is composed of two-hollowed cylinders. The outer cylinder represents the endmill tool, and the inner cylinder represents the damper. For convenience, the outer part (tool) is denoted as a shank, while the inner part (damper) is denoted as a finger. As schematically illustrated in Fig.3-2, the inner radius R1 of the finger is 1.5mm, the outer radius R2 of the finger is 4.7625mm, the inner radius R3 of the shank is 4.7625 mm, and the outer radius R4 of the shank is 9.525 mm. The length of the endmill is 101.6 mm. Because the gap between two contact surfaces is ignored, R2 is

equal to R3. R1 will be varied from 1.0 mm to 3.5 mm during the parameter study in chapter 6.

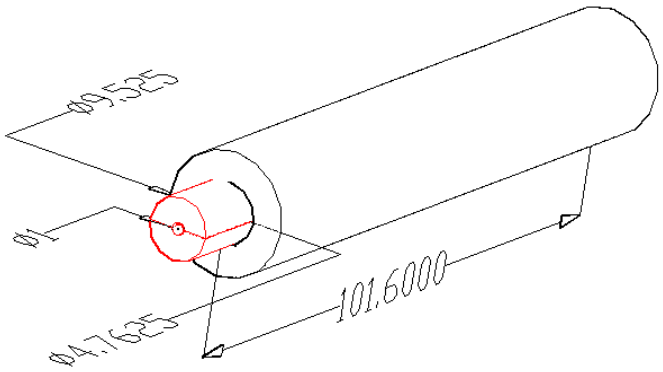

Figure 3-2. Dimensions of geometry

Although Fig.3-2 shows only two fingers, the number of fingers can be altered to improve the damping performance. The parameter study in chapter 6 will examine the effect of varying the number of fingers between 2 and 10. Because a damper with only one finger would have a lower contact pressure than the other cases, this case will not be considered.

Next, the operating condition is also simplified. The applied force is assumed to be sequential. It is first assumed that the tool is rotated with a constant angular velocity. The constant angular velocity will generate a constant contact force at the interface. For this particular model, an angular velocity of 2,722.713 rad/sec is used, which is equal to 26,000 rpm. In this initial state the endmill has not started cutting the surface. When the endmill starts cutting the surface, the tool undergoes a vertical force at the end of the endmill. To approximate the cutting process of the tool, a vertical force is applied at the tip. To accurately approximate the cutting force, the vertical force on the endmill needs to be measured and then an equal force needs be applied at the tip. However, since the objective of this research is vibration control, a representative force of 100N is applied.

Thus, the damping work that will be calculated is not the actual magnitude, but rather a relative quantity.

For simplicity, the same material properties are assumed for both the shank and finger .The material properties used are listed in Table 3-1.

Table 3-1. Material properties used for the shank and finger.

Material Property	Value
Young's Modulus	206780 MPa
Mass Density	$7.82 * 10^{-9} ton / mm^3$
Friction Coefficient	0.15

In the following chapters analytical and finite element analysis will use the simplified model to determine the conditions for maximum damping of the endmill.

Chapter 4

The Analytical Approach

Because it will provide a qualitative estimation of the numerical approach, it would be beneficial to review an analytical model before starting the finite element analysis. Sterling, a former researcher, developed an analytical method that can estimate the amount of friction work during chatter vibration. In this chapter, his analytical approach is reviewed and the results will be compared with finite element analysis results in chapter 5.

The work done by the friction force that occurs between the inner surface of the endmill and the outer surface of the damper causes the damping effect that reduces the chatter vibration. According to the Coulomb friction model, the friction force and the damping work can be written as follows:

$$\begin{aligned} F_f &= \mu \times N \\ W_f &= F_f \times U_f \end{aligned} \tag{4.1}$$

Where F_f is the friction force, μ is the friction coefficient, N is the normal contact force, W_f is the friction work, and U_f is the relative displacement between the two contact surfaces. The normal force N is mainly caused by the centrifugal force created when the endmill is rotating. The relative displacement U_f is mainly caused by the vertical deflection of the tool when the endmill starts cutting. Therefore, we can divide the endmill system into two states. The first state is when the endmill is rotating without any cutting operation. In this case, only the centrifugal force is applied. The second state is when the endmill starts cutting. In this state, the vertical force is added at the tip of the endmill. Both the centrifugal force and the vertical force are applied in this state. If we

assume that there is no relative motion in the first state, then we can calculate the work done by the friction force during the second state.

Calculation of the Normal Force and the Contact Pressure

In this section, the normal force and pressure that are caused by the rotational motion of the tool will be calculated. There are three assumptions for the the analytical method in this step. Those are listed as below.

- There is no angular acceleration, which means the angular velocity is constant.
- There is no relative motion between the two contact surfaces during the first step, which means there is no slip in the contact surface during the rotational motion.
- Contact occurs throughout the entire contact area during the second state. In the actual case, contact may not occur in some portions of the interface. For example there will be no contact near the fixed end or on the two sides where the neutral axis lies. All of these effects are ignored, and it is assumed that contact occurs throughout the entire area.

  Due to the second assumption, the contact pressure is calculated using the centrifugal force only and is assumed to remain constant. Now let us consider the simplified model, which was developed in chapter (Fig.3-2). The shank and the finger are hollowed cylinders. For simplicity, we only consider the case of a two-finger configuration. Figure 4-1(a) shows the cross-sectional area and dimensions of the endmill system in which two fingers are inserted. Considering the symmetric geometry of the fingers, we can consider one finger, which is illustrated in Fig.4-1 (b). Since the finger can have an arbitrary location, θ represents the start angle of the finger. The point G indicates the first moment

(centroid) of the finger's cross section, and R is the distance between the center of the tool and the centroid G. The normal force N and contact pressure P_c can then be obtained as,

$$N = MR\omega^2, \qquad P_c = \frac{MR\omega^2}{A_c} \tag{4.2}$$

Where A_c is the contact surface area, M is the mass of the finger, and ω is the angular velocity. The first step of calculating the contact pressure is to calculate the distance R, which is determined by the centroid of the finger's cross section.

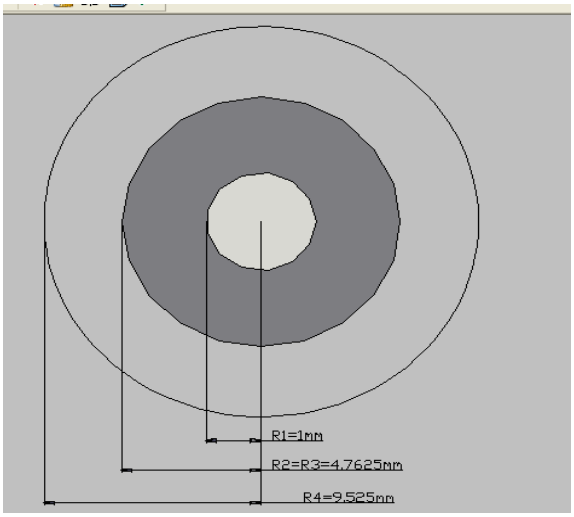

(a)

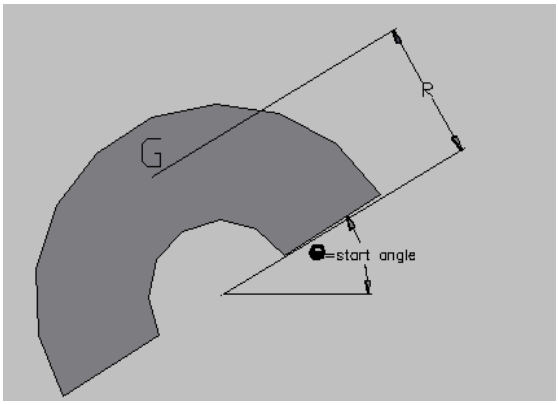

(b)

Figure 4-1. Cross sectional area of the endmill system. (a) Cross sectional area and dimension of the original model in which two fingers are inserted.(b) Cross sectional area of the finger. G is the mass center of the cross section, and θ is the start angle.

The centroid (first moment) of an assemblage of n similar quantities, $\Delta_1, \Delta_2, \Delta_3, ..., \Delta_n$ situated at point P_1, P_2, P_3,…, P_n for which the position vectors relative to a selected point O are r_1, r_2, r_3,…, r_n has a point vector $\bar{r}$ defined as

$$\bar{r} = \frac{\sum_{i=1}^{n} r_i \Delta_i}{\sum_{i=1}^{n} \Delta_i}$$

Where Δ_i is the i th quantity (for example, this could be the length, area, volume, or mass of an element), r_i is the position vector of i th element, $\sum_{i=1}^{n} \Delta_i$ is the sum of all n elements, and $\sum_{i=1}^{n} r_i \Delta_i$ is the first moment of all elements relative to the selected point O.

In terms of x, y, and z coordinates, the centroid has coordinates

$$\bar{x} = \frac{\sum_{i=1}^{n} x_i \Delta_i}{\sum_{i=1}^{n} \Delta_i}, \qquad \bar{y} = \frac{\sum_{i=1}^{n} y_i \Delta_i}{\sum_{i=1}^{n} \Delta_i}, \qquad \bar{z} = \frac{\sum_{i=1}^{n} z_i \Delta_i}{\sum_{i=1}^{n} \Delta_i},$$

Where Δ_i is the magnitude of the i th quantity (element), $\bar{x}, \bar{y}, \bar{z}$ are the coordinates of centroid of the assemblage, and x_i, y_i, z_i are the coordinates of P_i at which Δ_i is concentrated.

The centroid of a continuous quantity may be located through calculus by using infinitesimal elements of the quantity. Thus, for area A and in terms of x, y, z coordinates, we can write

$$\bar{x} = \frac{\int x dA}{\int dA} = \frac{Q_{yz}}{A}$$

$$\bar{y} = \frac{\int y dA}{\int dA} = \frac{Q_{xz}}{A}$$

$$\bar{z} = \frac{\int z dA}{\int dA} = \frac{Q_{xy}}{A}$$

where Q_{xy}, Q_{yz}, Q_{xz} are first moments with respect to the xy, yz, and xz planes, respectively. The following table indicates the first moments Q of various quantities Δ about the coordinate planes. In Table 4-1 Q_{xy}, Q_{yz}, Q_{xz} are first moments with respect to the xy, yz, and xz planes, L is the length, and m is the mass, respectively. Note that in two-dimensional work, e.g. in the xy plane, Q_{xy} becomes Q_x, and Q_{yz} becomes Q_y.

Table 4-1. First moment Q of various quantities.

Δ	Q_{xy}	Q_{yz}	Q_{xz}	Dimensions
Line	$\int z dL$	$\int x dL$	$\int y dL$	L^2
Area	$\int z dA$	$\int x dA$	$\int y dA$	L^3
Volume	$\int z dV$	$\int x dV$	$\int y dV$	L^4
Mass	$\int z dm$	$\int x dm$	$\int y dm$	mL

Now let us consider the case illustrated in Fig.4-2, which is a cross section of the finger. According to the figure, $\bar{y}$ can be expressed as

$$\bar{y} = R = \frac{\int y dA}{\int dA} = \frac{Q_x}{A}$$

If we choose the polar coordinate system y is represented by,

$$y = r\cos\theta$$

Using this polar coordinate system, the $\bar{y}$ of the centroid can be calculated by,

$$\bar{y} = \frac{Q_x}{A} = \frac{\int y dA}{\int dA} = \frac{\int_{\alpha}^{\beta}\int_{R_1}^{R_2} r\cos(\theta) r dr d\theta}{\int_{\alpha}^{\beta}\int_{R_1}^{R_2} r dr d\theta}$$

$$= \frac{\left[\frac{1}{3}r^3\right]_{R_1}^{R_2}\int_{\alpha}^{\beta}\cos(\theta)\, d\theta}{\left[\frac{1}{2}r^2\right]_{R_1}^{R_2}\int_{\alpha}^{\beta} d\theta}$$

$$= \frac{2(R_2^3 - R_1^3)}{3(R_2^2 - R_1^2)}\frac{\sin(\beta)+\sin(\alpha)}{\beta-\alpha}$$

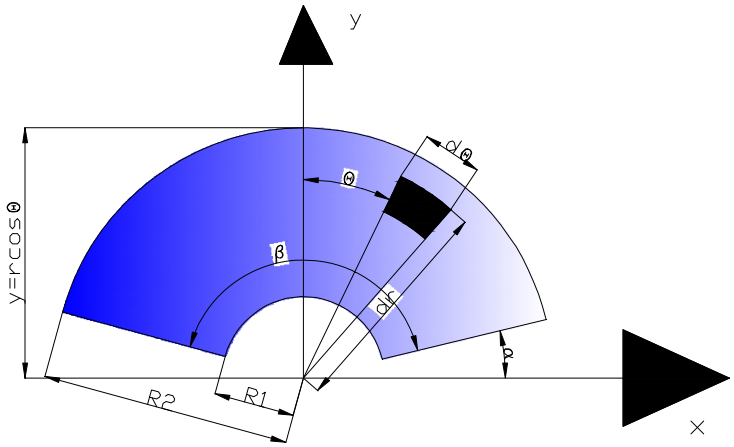

Figure 4.3: Cross-sectional area of the finger.

If $\alpha = 0$,

$$\bar{x} = \frac{2(R_2^{\,3} - R_1^{\,3})}{3\left(R_2^{\,2} - R_1^{\,2}\right)} \frac{\sin(\beta)}{\beta}$$

Since the centroid of the cross section is always located along the symmetric line of the finger, it is convenient if the y-axis is chosen such that the centroid is located on the y-axis, as illustrated in Fig.4-3. Due to the symmetry, the integration of the domain can be done between $-\alpha$ and α for angles, which provides a convenient formula. If we choose the polar coordinate system, from the Fig.4-3, y is represented by,

$$y = r\cos\theta$$

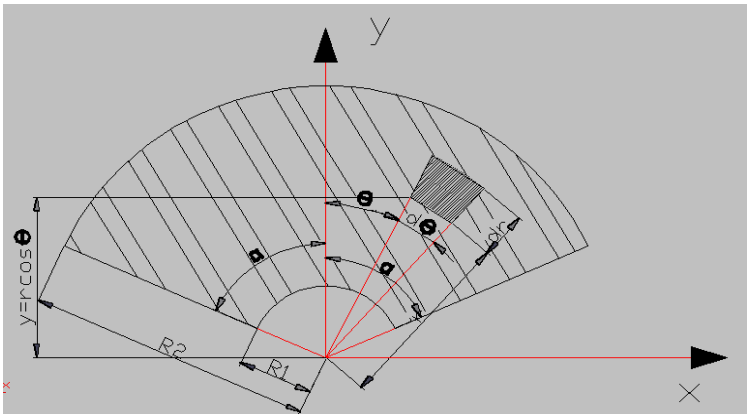

Figure 4-3. Cross sectional area of the finger.

Using this polar coordinate system, the $\bar{y}$ of the centroid can be calculated by,

$$\bar{y} = \frac{Q_x}{L} = \frac{\int y dA}{\int dA} = \frac{\int_{-\alpha}^{\alpha}\int_{R_1}^{R_2} r\cos(\theta)\, r dr d\theta}{\int_{-\alpha}^{\alpha}\int_{R_1}^{R_2} r dr d\theta}$$

$$= \frac{\left[\frac{1}{3}r^3\right]_{R_1}^{R_2}\int_{-\alpha}^{\alpha}\cos(\theta)\, d\theta}{\left[\frac{1}{2}r^2\right]_{R_1}^{R_2}\int_{-\alpha}^{\alpha} d\theta}$$

$$= \frac{2(R_2^3 - R_1^3)}{3(R_2^2 - R_1^2)}\frac{\sin(\alpha)-\sin(-\alpha)}{\alpha-(-\alpha)}$$

$$= \frac{2(R_2^3 - R_1^3)}{3(R_2^2 - R_1^2)}\frac{\sin(\alpha)}{\alpha}$$

$$\therefore R = \frac{2(R_2^3 - R_1^3)}{3(R_2^2 - R_1^2)}\frac{\sin(\alpha)}{\alpha} \tag{4.3}$$

This equation can be used for the general case which undergoes the centrifugal force. For the simplified model in chapter 3, $\alpha = \frac{\pi}{2}$, R_2 = 4.7625mm, R_1=1.5mm.

Substituting these values into the above equation yields $\bar{y}$ = R = 2.1738mm. Substituting this value into Eq.(4.2) yields the normal force and the contact pressure between two contact surfaces. In Eq.(4.2), the contact area A_c can be calculated by

$$A_c = \pi R_2 L = \pi \times 4.7625 \times 101.6 = 1520\left[mm^2\right]$$

which assumes that all parts of the surface are in contact. Using the material properties shown in Table 2-1, the mass M can be calculated by

$$M = \rho V = 7.82 \times 10^{-6} \times \frac{\pi}{2}(4.7625^2 - 1.5^2) \times 101.6$$

$$= 2.5499 \times 10^{-2} \quad \text{kg.}$$

Therefore the contact pressure P_c can be obtained from Eq.(4.2), as

$$P_c = \frac{MR\omega^2}{A_c} = \frac{2.5499 \times 10^{-2} \times 2.1738 \times 2722.713^2}{1520}$$

$$= 270.33\left[KPa\right] = 0.2703\left[MPa\right]$$

It is noted that the contact pressure P_c is calculated from the assumption that the whole surface is in contact with a constant pressure.

Calculation of the Relative Displacement and the Work

In this section the relative displacement that is caused by the vertical force (cutting force) will be calculated and the work that has been done by the friction force will be calculated. This state represents the one in which the endmill starts the cutting operation. The same assumptions are used as in the last case except for the second one because there is now a relative motion between the two contact surfaces. The assumptions are:

- There is no angular acceleration, which means the angular velocity is constant.
- There is no normal contact force change caused by the vertical force.
- Contact occurs throughout the entire contact area.

Because the centrifugal force is dominant in this endmill system, the change of the normal contact force due to the vertical force is ignored in this step. The first step of calculating the frictional work is to obtain the second moment of inertia of the finger. The

following definitions of the second moment, or moment of inertia are analogous to the definitions of the first moment of a plane area, which were given in the previous section. The derivation of load-stress formulas for beams may require solutions of one or more of the following equations:

$$I_x = \int y^2 dA$$
$$I_y = \int x^2 dA \qquad (4.4)$$
$$I_{xy} = \int xy dA$$

where dA is an element of the plane area A lying in the x-y plane. A represents the cross sectional area of a member subjected to bending and/or torsional loads. The integrals in the above equations are commonly called moments of inertia of the area A because of the similarity with integrals that define the moment of inertia of bodies in the field of dynamics. From Eq.(4.4), if we choose the polar coordinate system, x and y are represented as,

$$x = r\cos\theta, \qquad y = r\sin\theta$$

And I_x, I_y, I_{xy} are

$$I_x = \int_{\alpha}^{\beta}\int_{R_1}^{R_2} r^3 \sin^2\theta dr d\theta = \frac{1}{8}(R_2{}^4 - R_1{}^4)(\beta - \alpha - \sin\beta\cos\beta + \sin\alpha\cos\alpha)$$

$$I_y = \int_{\alpha}^{\beta}\int_{R_1}^{R_2} r^3 \cos^2\theta dr d\theta = \frac{1}{8}(R_2{}^4 - R_1{}^4)(\beta - \alpha + \sin\beta\cos\beta - \sin\alpha\cos\alpha) \qquad (4.5)$$

$$I_{xy} = \int_{\alpha}^{\beta}\int_{R_1}^{R_2} r^3 \sin\theta\cos\theta dr d\theta = \frac{1}{8}(R_2{}^4 - R_1{}^4)(\sin^2\beta - \sin^2\alpha)$$

If $\alpha = 0$ the Eq.(4.5) can be written as

$$I_x = \int_0^{\alpha}\int_{R_1}^{R_2} r^3 \sin^2\theta dr d\theta = \frac{1}{8}({R_2}^4 - {R_1}^4)(\alpha - \sin\alpha\cos\alpha)$$

$$I_y = \int_0^{\alpha}\int_{R_1}^{R_2} r^3 \sin^2\theta dr d\theta = \frac{1}{8}({R_2}^4 - {R_1}^4)(\alpha + \sin\alpha\cos\alpha)$$

$$I_{xy} = \int_{\alpha}^{\alpha}\int_{R_1}^{R_2} r^3 \sin\theta\cos\theta dr d\theta = \frac{1}{8}({R_2}^4 - {R_1}^4)\sin^2\alpha \qquad (4.6)$$

For the simplified model in chapter 3, $\alpha = \pi$, R_1 =1.5mm, R_2=4.7625mm. Substituting those values into the above equation yields,

$$I_x == \frac{1}{8}(4.7625^4 - 1.5^4)(\pi - \sin\pi\cos\pi) = \frac{\pi}{8}(4.7625^4 - 1.5^4)$$

Thus, the moment of inertia of the upper finger is

$$I_x = \frac{\pi}{8}({R_3}^4 - {R_4}^4) = \frac{\pi}{8}(4.7625^4 - 1.5^4) = 200\left[mm^4\right]$$

The moment of inertia of the lower finger can be obtained in the same way because the two fingers are symmetric about the x-axis, and the two values would be the same.

Now let us calculate the relative displacement and the friction work. It is well known that beams undergo internal shear deformations along their axes during bending. Members of a composite beam that are not securely fixed together will slide over each other in proportion to their distance from the neutral axis of entire composite beam. It is known that for a cantilevered beam with a point load at the end, the vertical deflection at any point in the beam's neutral surface is

$$\delta = \frac{F}{6EI}(-x^3 + 3xL^2 - 2L^3)$$

where F is the force on the end of the beam, E is the beam's elastic modulus, I is the beam's moment of inertia, x is the position along the length of the beam measured from the free end, and L is the length of the beam.

If a composite beam is bent, all members will have the same deflection at the tip. Therefore it can be written that

$$\delta = \frac{F_s}{6E_s I_s}(-x^3 + 3xL^2 - 2L^3) = \delta = \frac{F_f}{6E_f I_f}(-x^3 + 3xL^2 - 2L^3) \qquad (4.7)$$

where, subscript s means the shank, and f means the finger. The external force F at the tip of the endmill must equal the sum of the forces required to deflect each member.

$$F = F_s + \sum F_f \qquad (4.8)$$

If there are only two fingers inside the shank Eq.(4.7) can be written as

$$\frac{F_s}{E_s I_s} = \frac{F_{f1}}{E_{f1} I_{f1}} = \frac{F_{f2}}{E_{f2} I_{f2}}$$

The above equation can be written as follows

$$F_s = \frac{F_{f1} E_s I_s}{E_{f1} I_{f1}}, \text{ and } F_{f2} = \frac{F_{f1} E_{f2} I_{f2}}{E_{f1} I_{f1}}$$

Substituting these equations into (3.8) yields

$$F = F_s + F_{f1} + F_{f2} = \frac{F_{f1} E_s I_s}{E_{f1} I_{f1}} + F_{f1} + \frac{F_{f1} E_{f2} I_{f2}}{E_{f1} I_{f1}}$$

Solving the above equation for F_{f1} yields

$$F_{f1} = \frac{F E_{f1} I_{f1}}{(E_s I_s + E_{f1} I_{f1} + E_{f2} I_{f2})}$$

This equation can be reduced to

$$F_{f1} = \frac{F E_{f1} I_{f1}}{E_s I_s + \sum_{i=1}^{n} E_{fi} I_{fi}}$$

The same operation for F_s and F_{f2} yields

$$F_s = \frac{FE_sI_s}{E_sI_s + \sum_{i=1}^{n} E_{fi}I_{fi}}$$

$$F_{f2} = \frac{FE_{f2}I_{f2}}{E_sI_s + \sum_{i=1}^{n} E_{fi}I_{fi}}$$

The normal stress at any point in a cantilevered beam is given by

$$\sigma = \frac{Fxc}{I}$$

where σ is the stress, F is the force on the free end, x is the position along the beam measured from the free end, c is the distance from the beam's neutral axis to the point of interest, and *I* is the area moment of inertia of its cross section. The axial strain in the beam is then

$$\varepsilon = \frac{\sigma}{E} = \frac{Fxc}{EI}$$

Where ε is the axial strain and E is the Young's Modulus of the material. c is the sum of the quantity (d+y) where d is the distance of the neutral axis of the finger from the neutral axis of the composite beam and y is the perpendicular distance from the point in question to the neutral axis of the finger.

For any point in any component member of the composite beam, the change in position of the point related to x=0 (the free end of the beam) can be written as

$$\delta_{axial} = \int_0^x \varepsilon dx$$

Substituting the previously obtained equations into this integral for both the fingers and the shank, the following equations are obtained. The value of d of the finger can be represented by $R \times \sin\theta$, where θ is the start angle. Note that in the equation for the shank, d is zero because its neutral axis lies on the neutral axis of the composite beam.

$$\delta_{axial} = \int_x^L \frac{F \times x \times (d+y)}{EI} dx = \frac{FE_s I_s}{E_s I_s + \sum_{i=1}^{n} E_{fi} I_{fi}} \frac{(0+y)}{2E_s I_s} (L^2 - x^2) = \frac{F \times y \times (L^2 - x^2)}{2\left(E_s I_s + \sum_{i=1}^{n} E_{fi} I_{fi} \right)}$$

$$\delta_{faxial} = \int_x^L \frac{F \times x \times (d+y)}{EI} dx = \frac{FE_{fi} I_{fi}}{E_s I_s + \sum_{i=1}^{n} E_{fi} I_{fi}} \frac{(d+y)}{2E_{fi} I_{fi}} (L^2 - x^2) = \frac{F \times (d+y) \times (L^2 - x^2)}{2\left(E_s I_s + \sum_{i=1}^{n} E_{fi} I_{fi} \right)}$$

The relative displacement can then be obtained by subtracting the above two equations

$$\delta_{faxial} - \delta_{saxial} = \frac{F \times (d+y) \times (L^2 - x^2)}{2\left(E_s I_s + \sum_{i=1}^{n} E_{fi} I_{fi} \right)} - \frac{F \times y \times (L^2 - x^2)}{2\left(E_s I_s + \sum_{i=1}^{n} E_{fi} I_{fi} \right)} = \frac{F \times d \times (L^2 - x^2)}{2\left(E_s I_s + \sum_{i=1}^{n} E_{fi} I_{fi} \right)}$$

The work done through this displacement is by friction. The amount of work done is equal to the integral solved over the entire length of the beam of the frictional force (friction coefficient times the normal force, which is the force/unit length at a point times the differential length) multiplied by the relative displacement. Writing this equation (assuming the pressure, p, is uniform over the entire area of the finger)

$$\mu P(\delta_{faxial} - \delta_{saxial}) = \int_0^L \mu P \frac{F \times d \times (L^2 - x^2)}{2\left(E_s I_s + \sum_{i=1}^{n} E_{fi} I_{fi} \right)} dx$$

The work done by friction for a displacement of the end of the beam by a specified force, F, is then

$$W = \frac{1}{3} L^3 \mu P F \frac{d}{\left(E_s I_s + \sum_{i=1}^{n} E_{fi} I_{fi} \right)} \tag{4.9}$$

This equation helps us to plot work done by friction force for varying start angles with change of inner radius of finger and number of damper finger with the help of MATLAB the code of which is shown in the Appendix.. The plots show the results of the theoretical analysis.

Figure 4-4 is the work according to the change of the inner radius of the finger. As the radius increases the work decreases because the mass decreases. When the radius is 1.5mm and the number of finger is 2, the work done by the friction force is 7.1182J

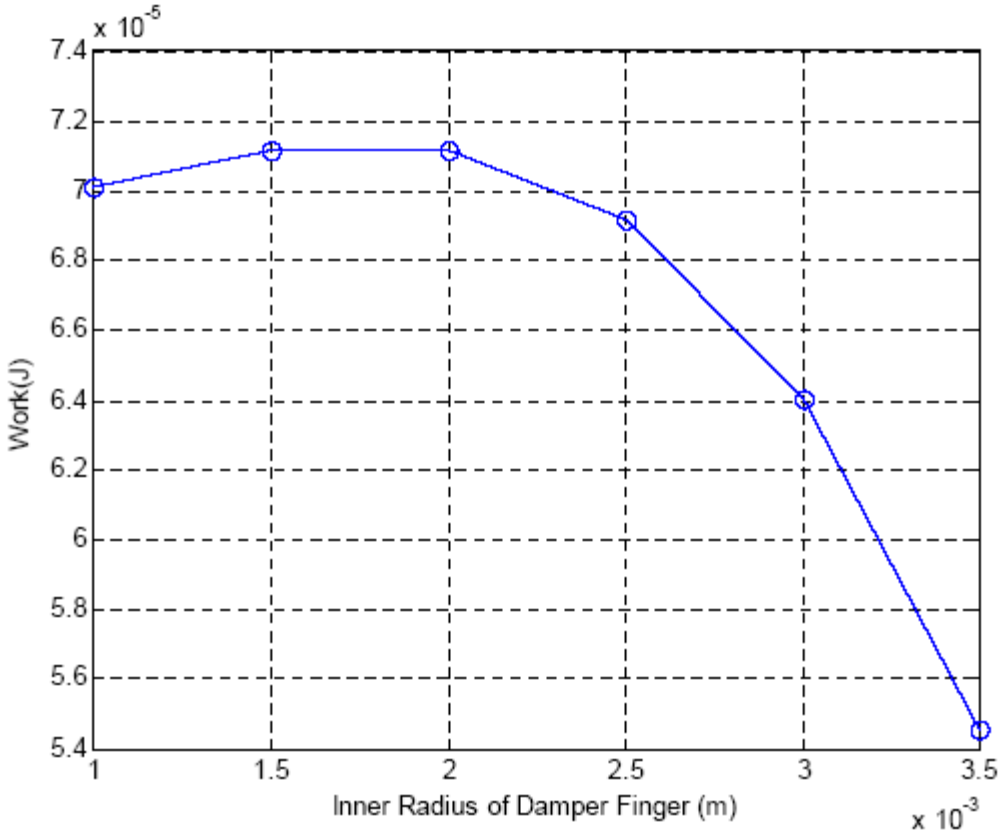

Figure 4-4. Plot of work done by the friction force according to the change of the inner radius of finger.

Figure 4-5 is the work calculated for different values of the start angle when the number of damper fingers is two and the inner radius is 1.5 mm. When the start angle is 0 it has its maximum value and this value gradually decreases as the angles decrease. Even when the number of fingers is held constant, the damping values differ for different positions of the finger. This result is reasonable because the relative displacement is zero at the neutral axis. In Chapter 6 this effect will be discussed in more detail.

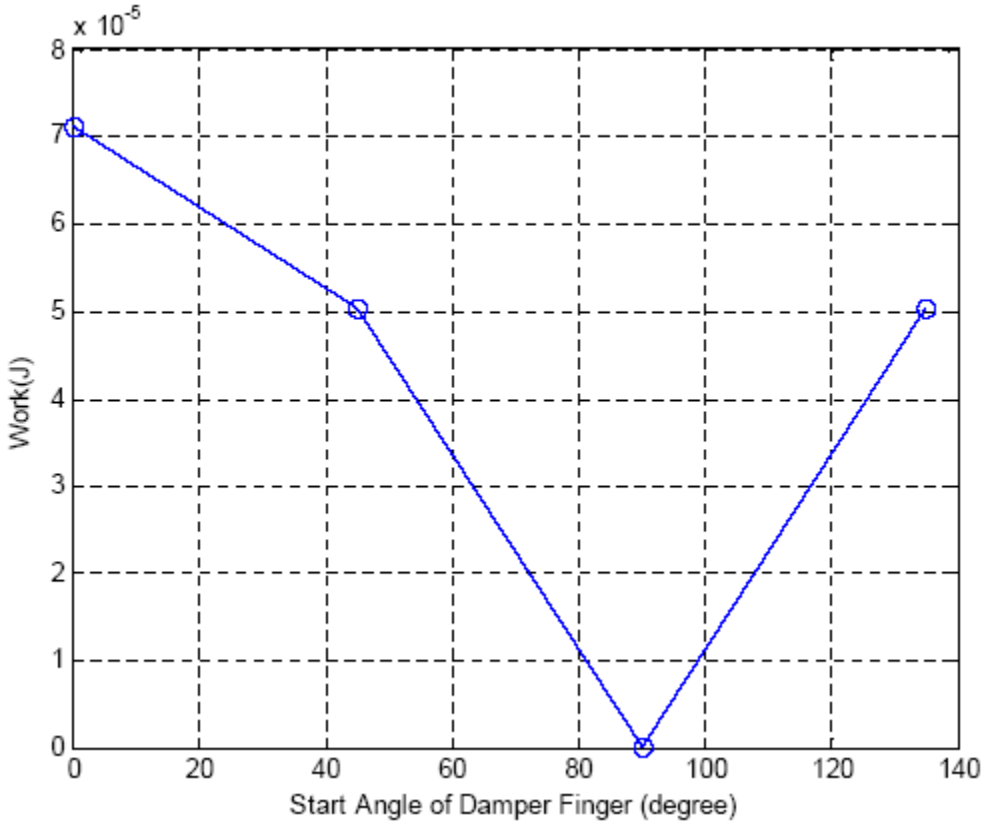

Figure 4-5. Plot of work done by the friction force for varying start angles of the finger. The radius of the finger is 1.5 mm and the number of the finger is 2.

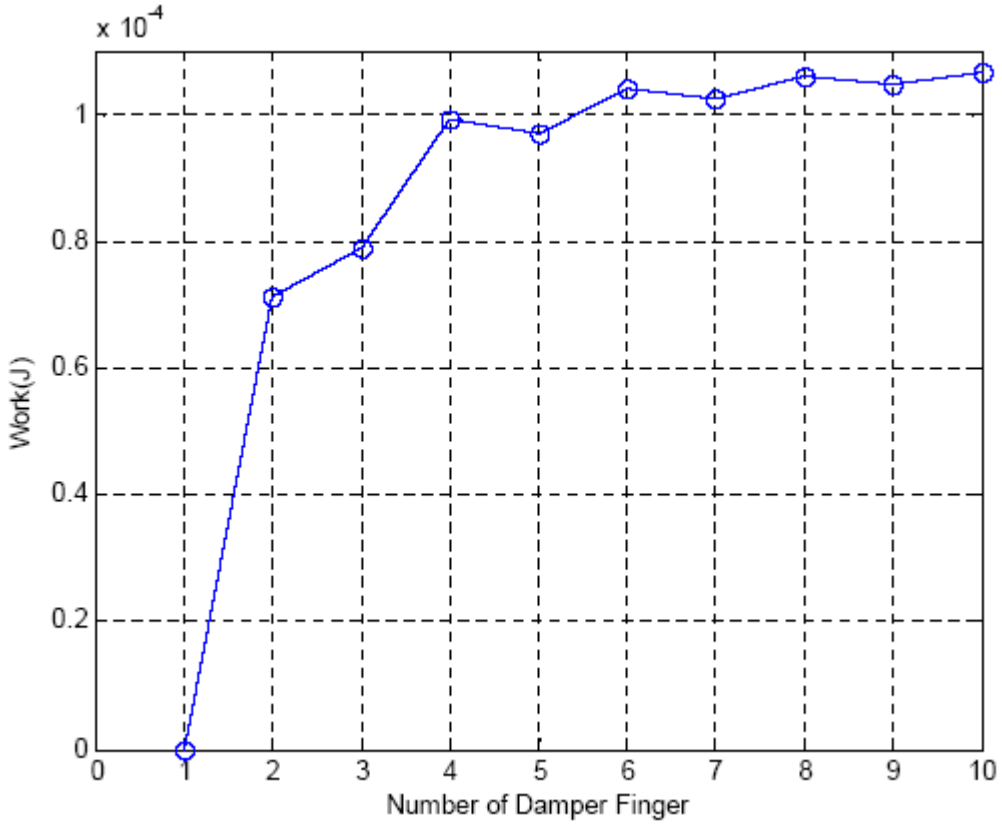

Figure 4-6. Plot of the work done by the friction force for different numbers of damper fingers. The inner radius of the finger is 1.5 mm and the start angle is chosen to have the maximum damping in each number of the finger.

Figure 4-6 shows the work for different numbers of fingers. The inner radius of the finger is 1.5 mm and the start angle is chosen to have the maximum damping for the number of fingers being used. The work increases gradually as the number of fingers is increased. Finite element analysis will be done for these analytical results in the following chapter.

Chapter 5

Finite Element Analysis

In this chapter, the finite element analysis procedure and results of the end-mill system are presented. Even though the cutting process is dynamic, a static finite element analysis is performed with the centrifugal force and the cutting force at the tip. Thus, the friction work obtained must be interpreted as a qualitative measure. Since the simulation condition is the same as that of the analytical method in chapter 3, it is still valid to compare the results of finite element analysis with the analytical results.

Modeling of the Shank and Finger

The first step of finite element analysis is to build a computational model. The simplified geometry for the end-mill in chapter 3 is used in FEA. Using the same material properties listed in Table2-1, 20-node solid elements in ANSYS (solid95) are use to build the shank and finger. Figure 5.1 illustrates a 20-node solid element that is used in ANSYS and figure 5.3 depicts the procedure of defining the element type. Figure 5.2 is a plot of the finite element model of the end-mill with boundary conditions.

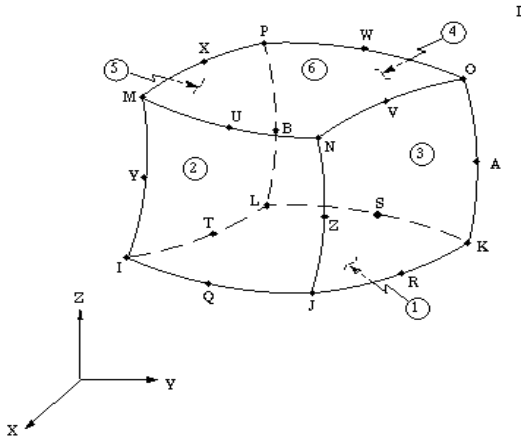

Figure 5-1: SOLID95, 20-node solid element.

Element Type Specification

ANSYS offers CONTA174 and TARGE170 for contact and target elements, "target" surfaces and a deformable surface, defined by this element. The element is applicable to 3-D structural and coupled thermal-structural contact analysis. This element is located on the surfaces of 3-D solid or shell elements with mid-side nodes. It has the same geometric characteristics as the solid or shell element face with which it is connected. Contact occurs when the element surface penetrates one of the target segments elements on a specified target surface.

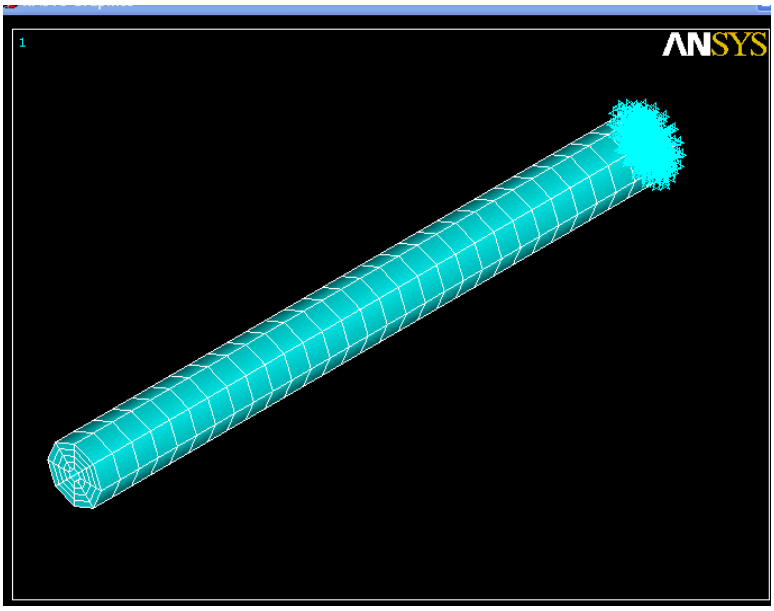

Figure 5.2: FEA model of the end-mill using 20 node cubic elements and 8 node contact elements with boundary condition.

SOLID95 is a higher order version of the 3-D 8-node solid element SOLID45. It can tolerate irregular shapes without as much loss of accuracy. SOLID95 elements have compatible displacement shapes and are well suited to model curved boundaries. The element is defined by 20 nodes having three degrees of freedom per node: translations in the nodal x, y, and z directions. The element

may have any spatial orientation. SOLID95 has plasticity, creep, stress stiffening, large deflection, and large strain capabilities.

To define the element type, open the following windows (figure 5.3a and 5.3b) and select the respective elements.

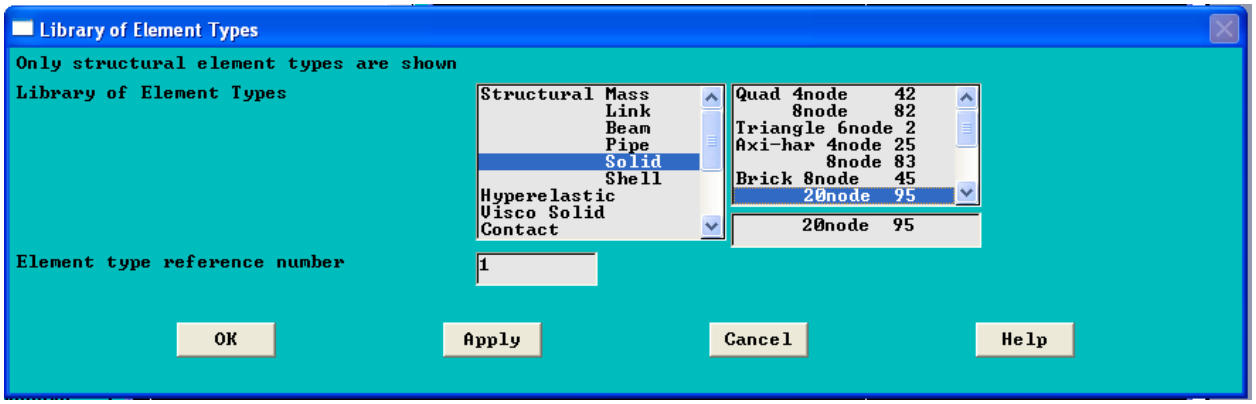

Figure 5.3a: Adding solid95 element type.

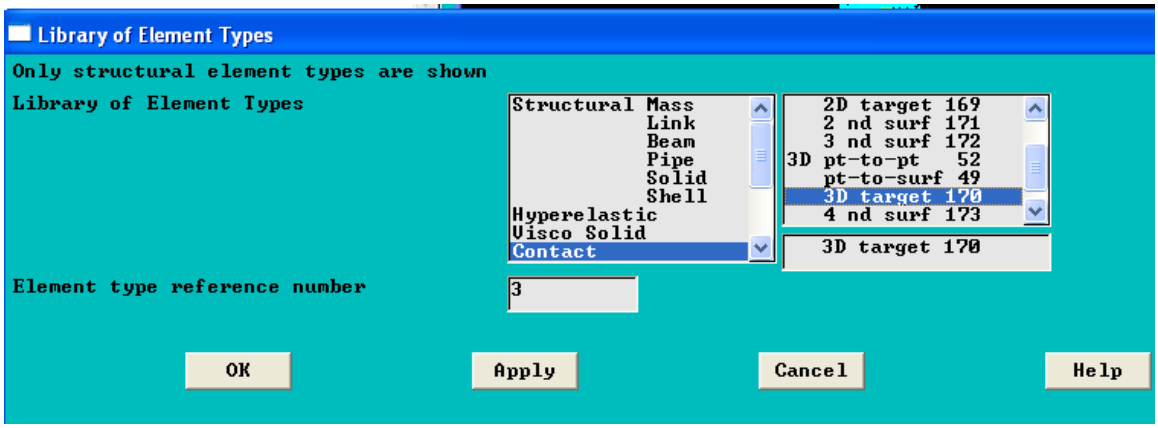

Figure 5.3b: Adding Contact/3D-target170 element type.

TARGE170 is used to represent various 3-D "target" surfaces for the associated contact elements (CONTA173, CONTA174, CONTA175, and CONTA176). The contact elements themselves overlay the solid elements describing the boundary of a deformable body and are potentially in contact with the target surface, defined by TARGE70. This target surface is discretized by a set of target segment elements (TARGE170) and is paired with its associated contact surface via a shared real constant set. Any translational or rotational displacement,

temperature, voltage, and magnetic potential on the target segment element can be imposed. Forces and moments on target element can also be imposed. To represent 2-D target surfaces, use TARGE169, a 2-D target segment element.

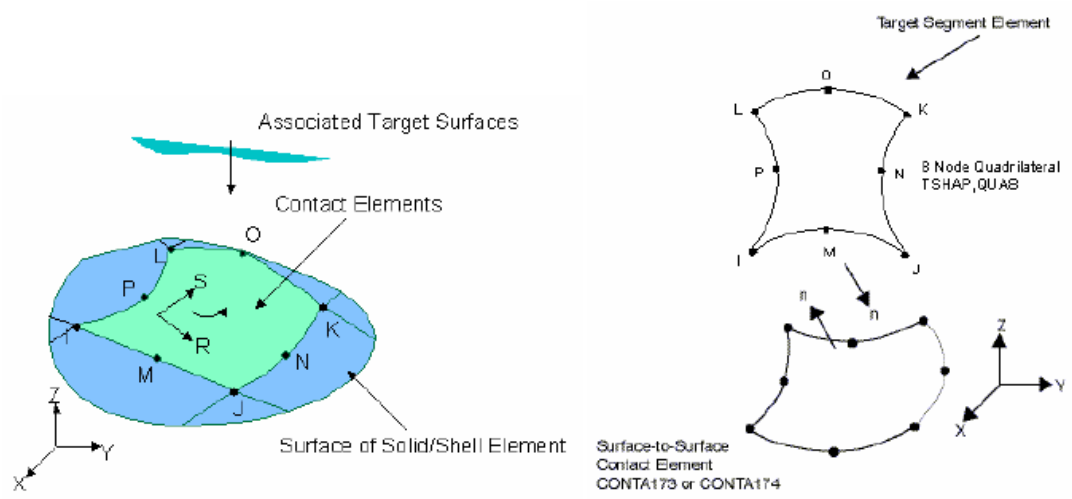

Figure 5-4: 8-node contact (CONTA174) and target (TARGE170) element description.

The target surface can either be rigid or deformable. For modeling rigid-flexible contact, the rigid surface must be represented by a target surface. For flexible-flexible contact, one of the deformable surfaces must be overlaid by a target surface.

For general 3-D rigid surfaces, target segment elements can be defined by area meshing (AMESH). For 3-D rigid lines, target segment elements can be defined by line meshing (LMESH). If the TARGE170 elements will be created via program meshing (AMESH, LMESH, or KMESH commands), then the TSHAP command is ignored and ANSYS chooses the correct shape automatically.

Since the contact area is curved, higher order elements must be used to prevent inaccurate representation of the surface. Since the contact element is defined on the surface of solid elements, the consistent order of the element must be used for the structure and contact surface. The counter part of SOLID95 structural

element is 8-node contact element, as illustrated in Fig.5-4. The contact elements are defined between the shank and finger.

Boundary Conditions

According to the forces applied to the end-mill, we can divide the analysis procedure into two steps.

***Step 1*:-** The first step is when the end-mill starts rotating. In this step, only the angular velocity of 2500rad/sec is applied without considering the cutting force.

***Step 2*:-** The second step is when the end-mill starts the cutting process. At this time a vertical force of 100 N is applied at the tip of the end-mill.

Calculation of Friction Work

It is known that damping can be calculated from:

$$\vec{\varsigma} = \vec{F}_f . \vec{S}$$

Where, $\vec{\varsigma}$ =damping,

$\vec{F}_f$ =Friction force,

$\vec{S}$ = Slide (Relative displacement)

After finishing FEA, the damping work which is done by the friction force is calculated. First, the friction stress and the relative slide in each contact element are obtained for each load step. By assuming a constant stress within an element, the friction force can be obtained by multiplying the friction stress with the element area. The dot product of the friction force vector and the relative displacement vector in each sub-step and in each element yields the friction work.

Finite Element Analysis Results

Load Step 1: When only angular velocity is applied.

Figure 5-5(a-d) is the results at load step 1 when only the angular velocity is applied. In Chapter 4, the analytical method estimates the contact pressure to be

0.27MPa. Where as, the maximum contact pressure from FEA is 0.58MPa, as shown in figure 5.5b.

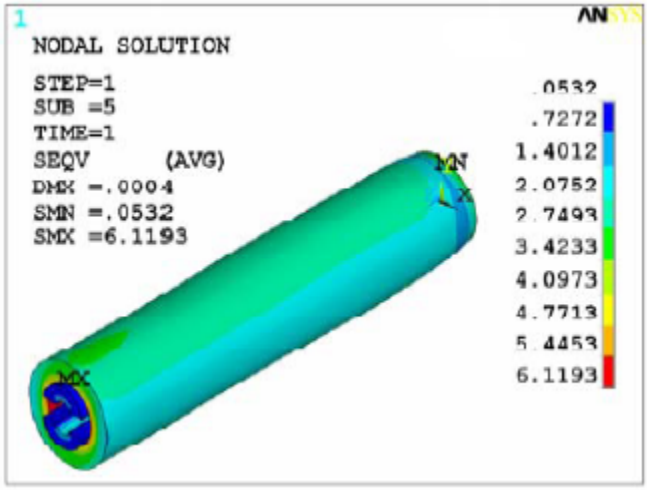

(a)

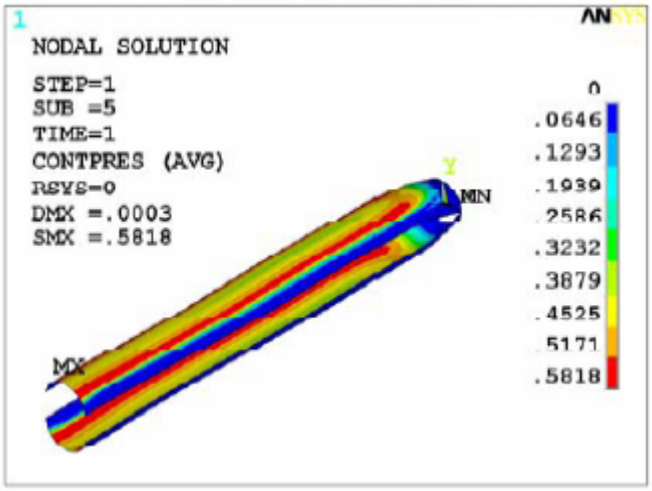

(b)

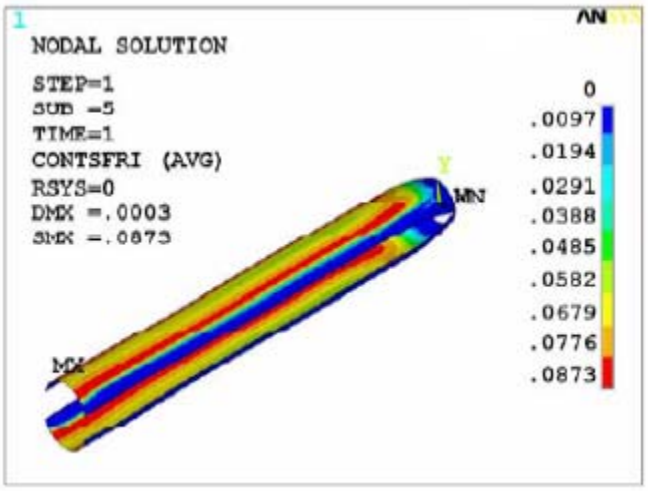

(c)

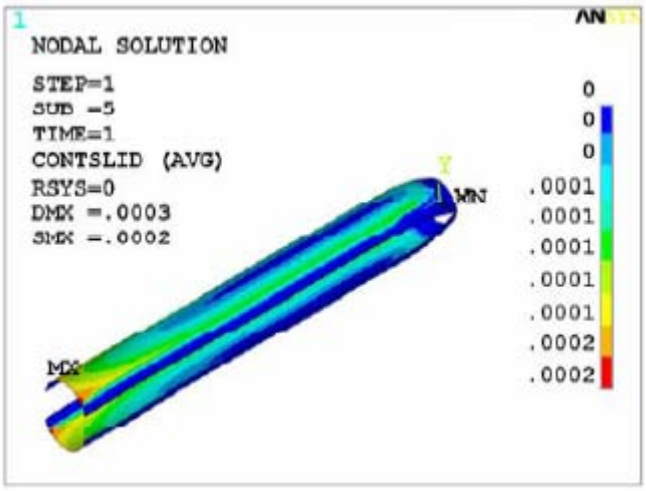

(d)

Figure 5-5: FEA result for load step 1 when only the angular velocity is applied. (a) is the von misses stress (MPa), (b) is the contact pressure (MPa), (c) is the frictional stress (MPa), and (d) is the slide (mm) . MX indicates where the maximum value and MN means the minimum value.

Since the actual contact occurs only half of the contact surface, the higher contact pressure from FEA is expected. In addition, the contact pressure is not constant: maximum at the top and the bottom surface and zero at both sides. Even though we assume that there is no relative motion between the contact

surfaces during load step 1 in Chapter 4, there is a relative motion due to the diameter change. However, the relative motion in load step 1 should not be counted because it is not related to the chatter vibration.

Load Step 2 (Centrifugal Force + Vertical Force)

In the load step 2, a vertical force (cutting force) is applied on top of the centrifugal force. Figure 5-6 shows the results of load step 2. The frictional work is calculated by dot producing the friction force (Fig.5-6 (c)) and the relative slide (Fig.5-6(d)). Since the load step is divided into five sub steps, the friction work at each sub step must be summed. The total friction work during load step 2 is $3.3426 * 10^{-5}$ [J]. By comparing with the analytical results $7.1182 * 10^{-5}$ [J] in Chapter 4, the finite element analysis estimates about 50% of the analytical result. The friction work calculated from FEA is less than that from the analytical approach because the actual contact area is small in FEA. There is no contact on two sides: the neutral axis lies and the fixed end. In addition, the contact pressure is not constant. That is why the analytical result is about two times higher than the FEA result. Another interesting observation is that most of the relative displacement occurs on the bottom side of the finger (see Fig.5-6 (d)). That happens because the vertical force is applied to the top side of the end-mill.

Figure 5-7, a schematic diagram of end-mill bending according to the applied force, explains in more detail. This figure is exaggerated; the real deformation is very small. Fig.5-7 (a) shows the initial state. When the end-mill starts rotating, the centrifugal force is applied and the deformed shape looks like Fig.5-7 (b).

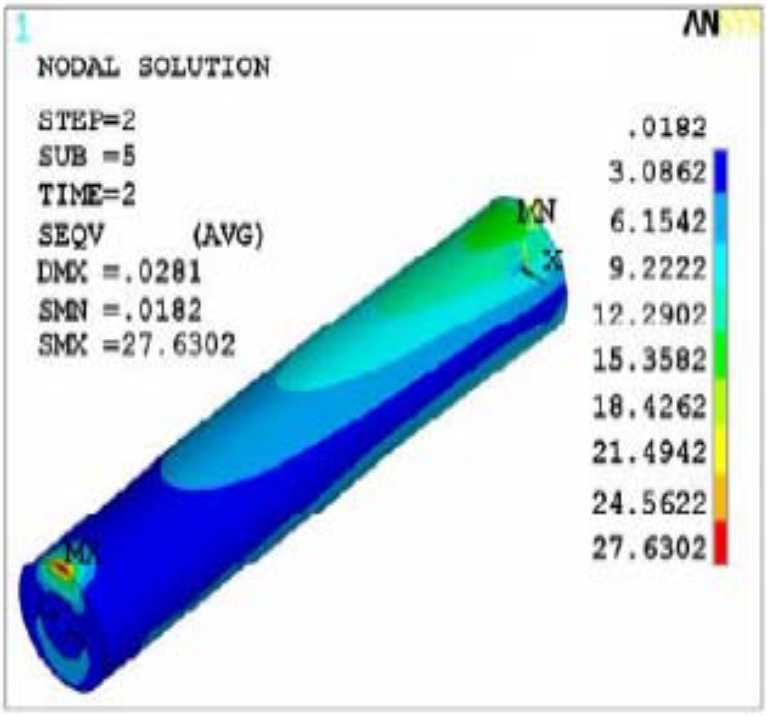
1
NODAL SOLUTION
STEP=2
SUB =5
TIME=2
SEQV (AVG)
DMX =.0281
SMN =.0182
SMX =27.6302
.0182
3.0862
6.1542
9.2222
12.2902
15.3582
18.4262
21.4942
24.5622
27.6302
MN
MX

(a)

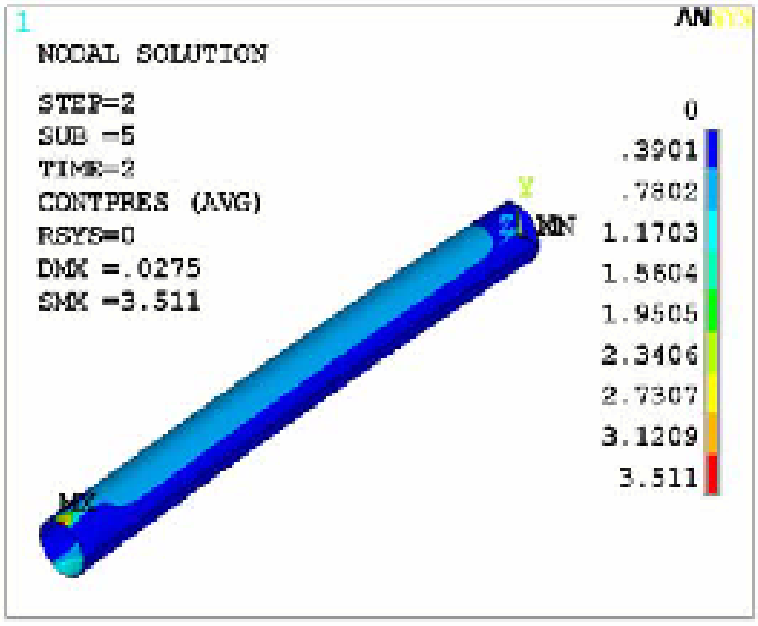
1
NODAL SOLUTION
STEP=2
SUB =5
TIME=2
CONTPRES (AVG)
RSYS=0
DMX =.0275
SMX =3.511
0
.3901
.7802
1.1703
1.5604
1.9505
2.3406
2.7307
3.1209
3.511
MN
MX

(b)

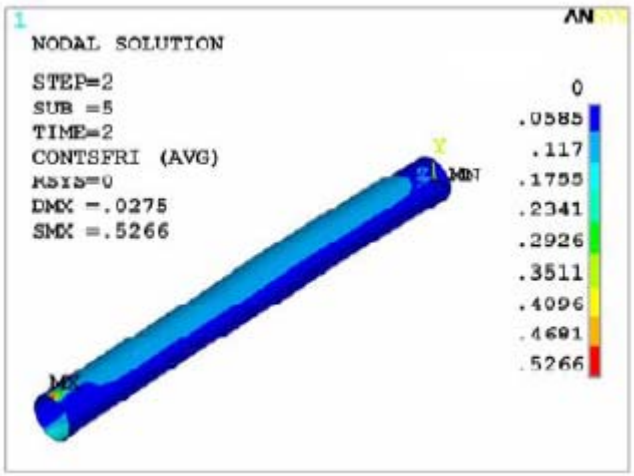

(c)

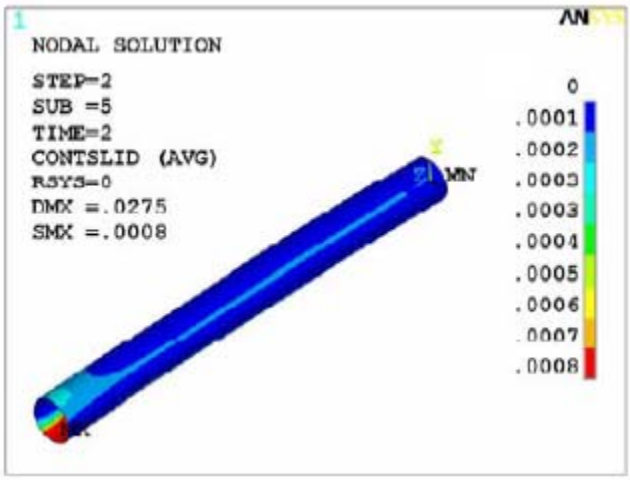

(d)

Figure 5-6: FEA result for load step 2 when both angular velocity and vertical forces applied. (a) The von-misses stress (MPa) (b) The contact pressure (MPa) (c) The frictional stress (MPa) (d) The slide (mm). MX indicates where the maximum value and MN means the minimum value.

Due to the mass conservation, the length of the shank reduces as the diameter increases. Where as, the length of the finger is not reduced because the

cylindrical finger is cut along its neutral axis. When the vertical load is applied on top of the centrifugal force, the shank and the finger are deformed, as illustrated in Fig.5-7 (c). Due to the difference in geometric center, the deflected shape has the largest slide at the bottom surface.

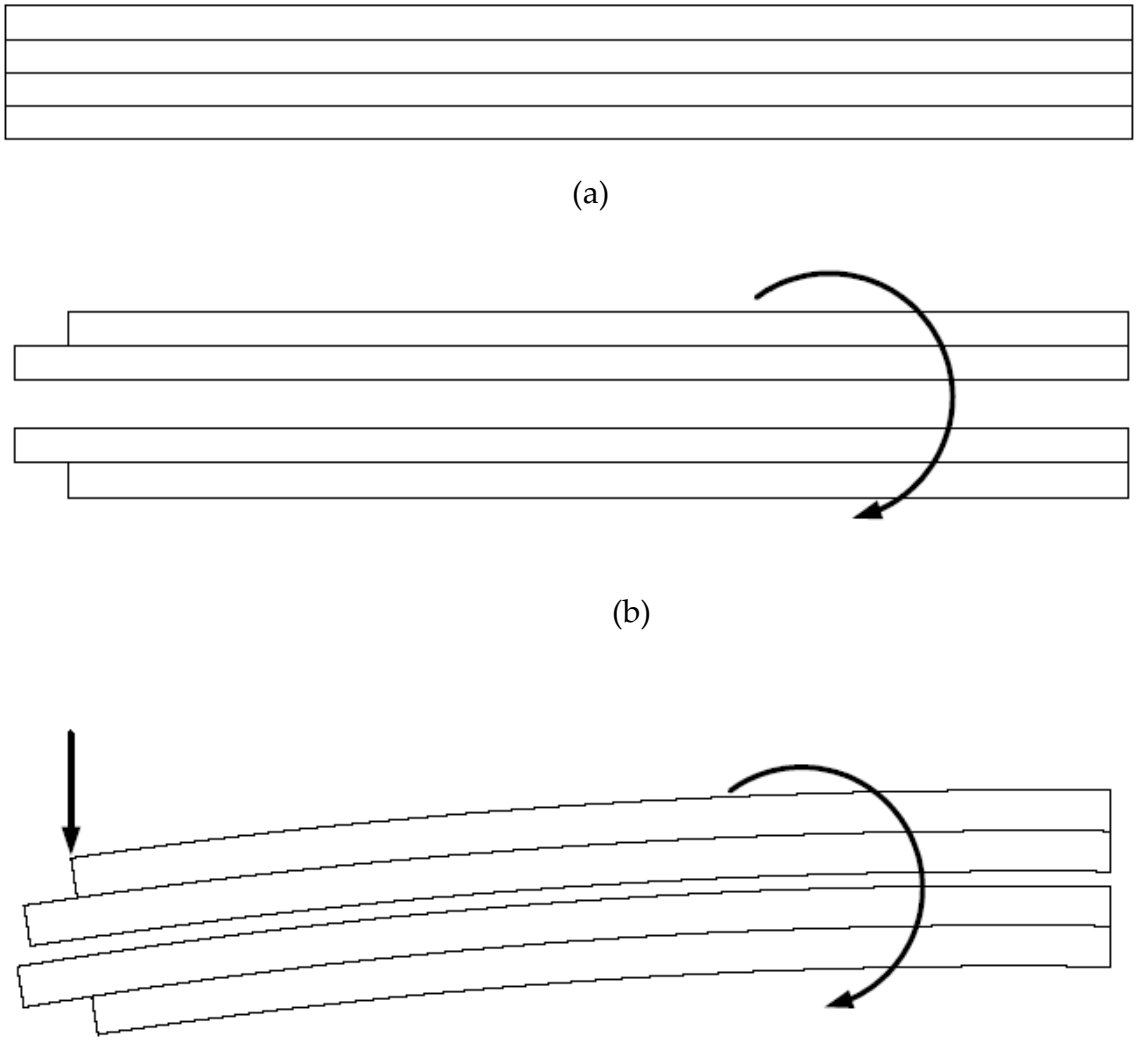

(a)

(b)

(c)

Figure 5-7: Schematic diagram of end-mill behavior according to the applied forces. (a) Shows the initial state, in (b) the angular velocity is applied and in (c) the vertical force is added.

Chapter 6

Result Analysis by variation of Parameters

In this chapter, a parameter study is performed to investigate the effect of damper design parameters on the friction work. Two design parameters: the inner radius of the finger and the number of fingers, are changed. The results of the parameter study are discussed with respect to the results of the analytical approach.

Determination of the Start Angle

Before starting the parameter study, a start angle must be chosen for different configurations. This is because the damping value changes with starting angle even if the same number of fingers is used.

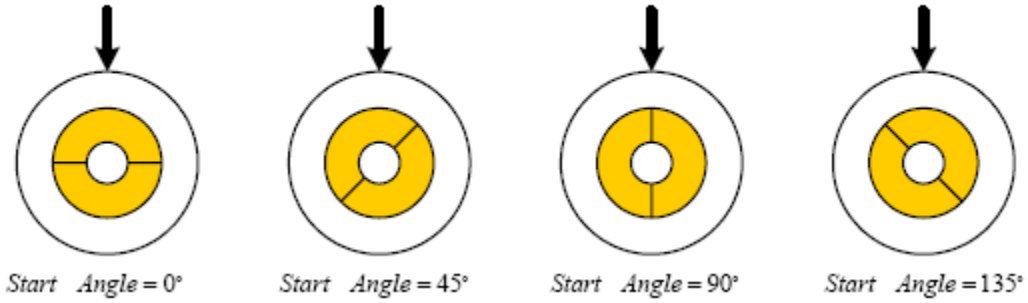

(a) Position of the finger for the two-finger case

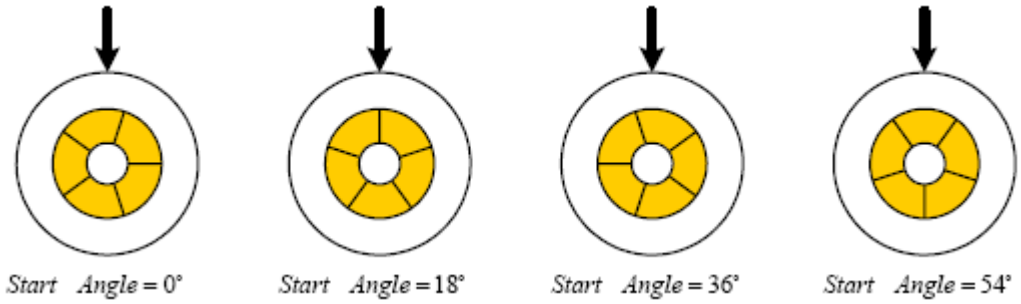

(b) Position of the finger for the five-finger case

Figure 6-1 Position of the finger

Let us consider the cases where the number of fingers is 2 and 5 more in detail. Figure 6-2 shows the relative displacement for the two-finger case. Figure 6-2 (a) and (b) show the case where the start angle of the finger is 90^0. Figure 6-2

(c) and (d) show the result when the start angle is 0^0. In both cases the pressure between the contact surfaces is almost the same for each position of the finger. But the relative displacement is different.

Figure 6.2 shows that most sliding occurs in the bottom part of the contact surface. That is because the force is applied at the top surface. If we use this relative displacement for calculating the frictional work, the work calculated when the start angle is 0^0 is bigger than90^0.

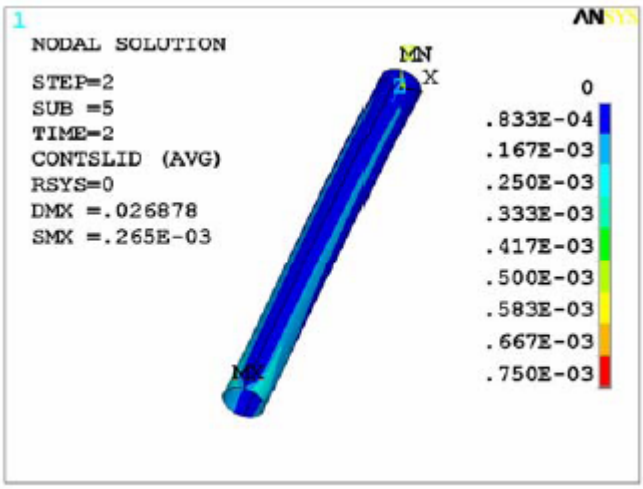

(a) Top

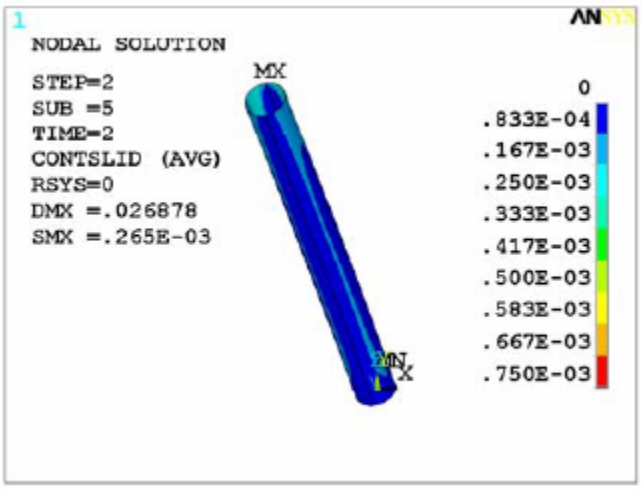

(b) Bottom

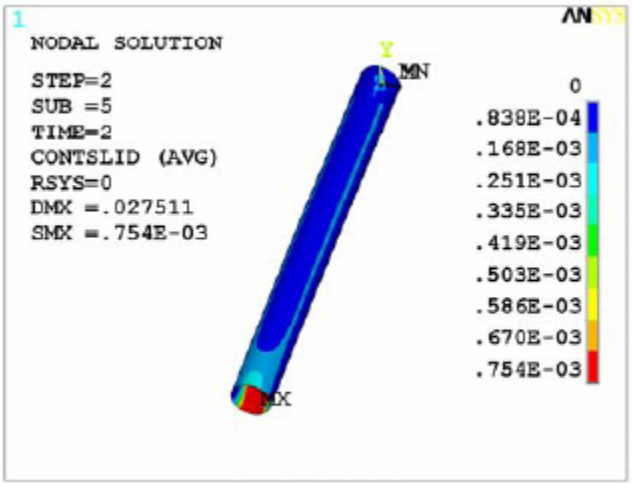

(c) Top

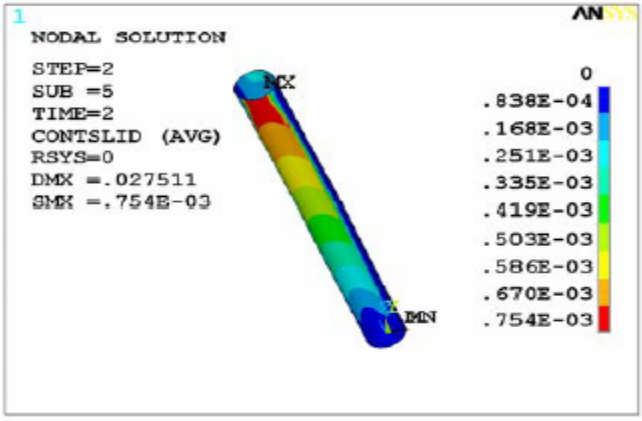

(d) Bottom

Figure 6-2: Relative displacement of the two-finger case. (a), (b) is when the start angle of the finger is 90^0, and (c), (d) is 0^0. MX indicates where the maximum value occurs and MN means the minimum value.

The figure shows that most sliding occurs in the bottom surface of the contact surface. This is because the force is applied at the top surface. If we use this relative displacement for calculating the frictional work, the work calculated when the start angle is 0^0 is greater than 90^0.

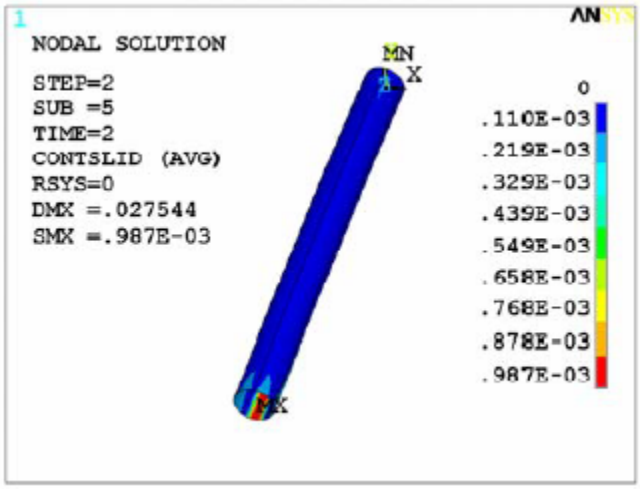

(a) Top

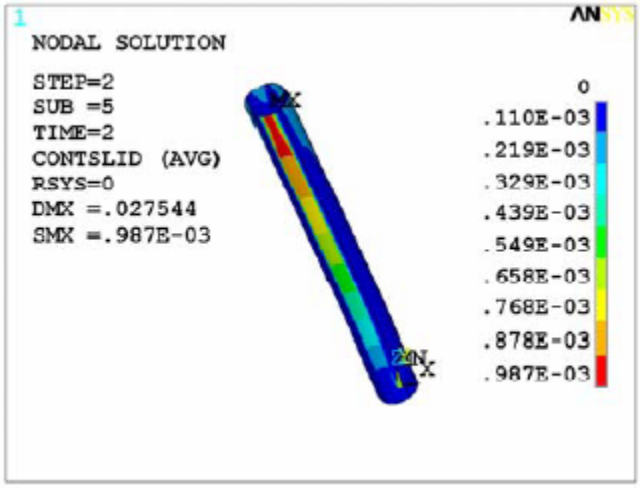

(b) Bottom

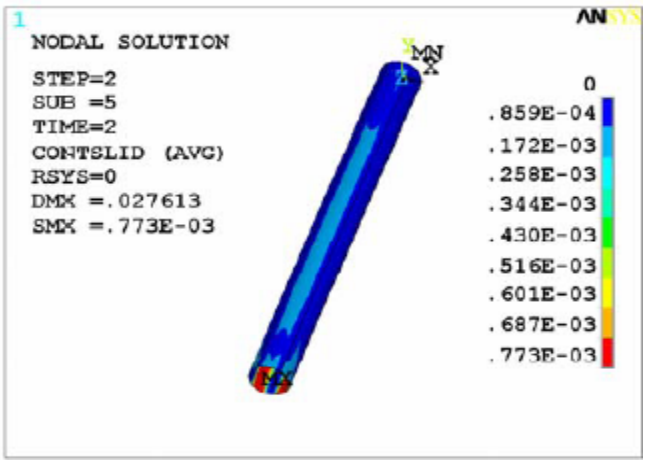

(c)Top

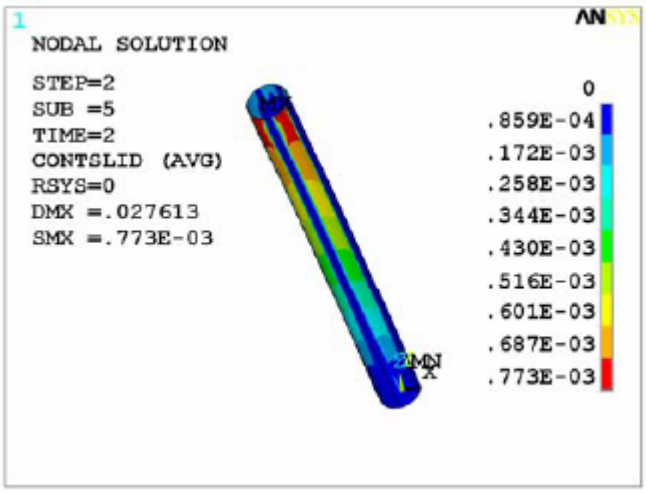

(d)Bottom

Figure 6-3: Relative displacement of five-finger case. (a), (b) is when the start angle of the finger is 18^0, and (c), (d) is 54^0 . MX indicates where the maximum value occurs and MN means the minimum value

The five-finger case is very similar to the two-fingered case. Figure 6-3 shows the five-finger case. Parts (a) and (b) are for a start angle of 18^0 and parts (c) and (d) are for a start angle of 54^0. If we compare Figure 6-3 (b) with Figure 6-3 (d), the latter has almost twice greater sliding region than the former. This is because the location of the finger differently affects the damping work.

Parameter Study

To find the maximum value of damping, a parameter study was done for two design variables. Figure 6-4 shows the first design variable, which is the inner radius of the finger, and Figure 6-5, the second design variable, the number of fingers.

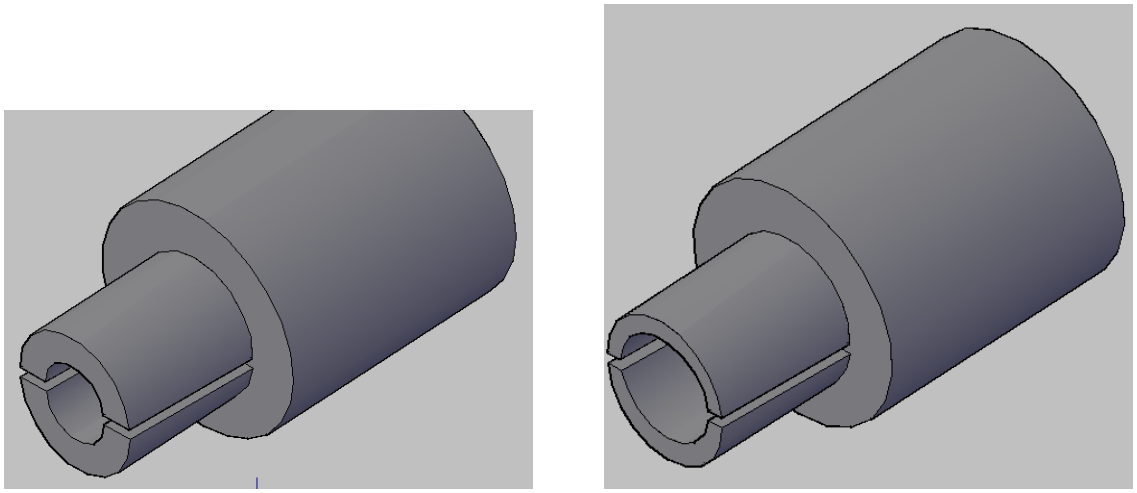

Figure 6-4: The first design parameter: the inner radius (R1) of the finger (varied from 1.5 mm to 3.5 mm).

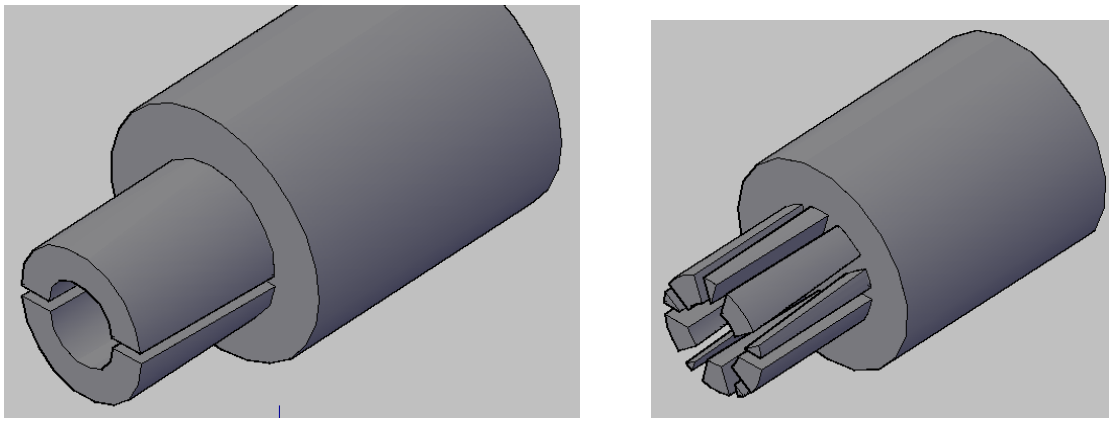

Figure 6-5: The second design variable: the number of fingers (from 2 to 10).

Change the Inner Radius of the Finger.

First the radius is changed from 1.0mm to 3.5mm for the two-finger case. Figure 6-6 shows the result. It's obvious that the work done by the friction force is gradually reduced, since the mass of the finger is reduced when the radius is increased. When the radius is 1.0mm the damping is 3.28×10^{-5}[J],and when the radius is 3.5mm it is2.53×10^{-5}[J].

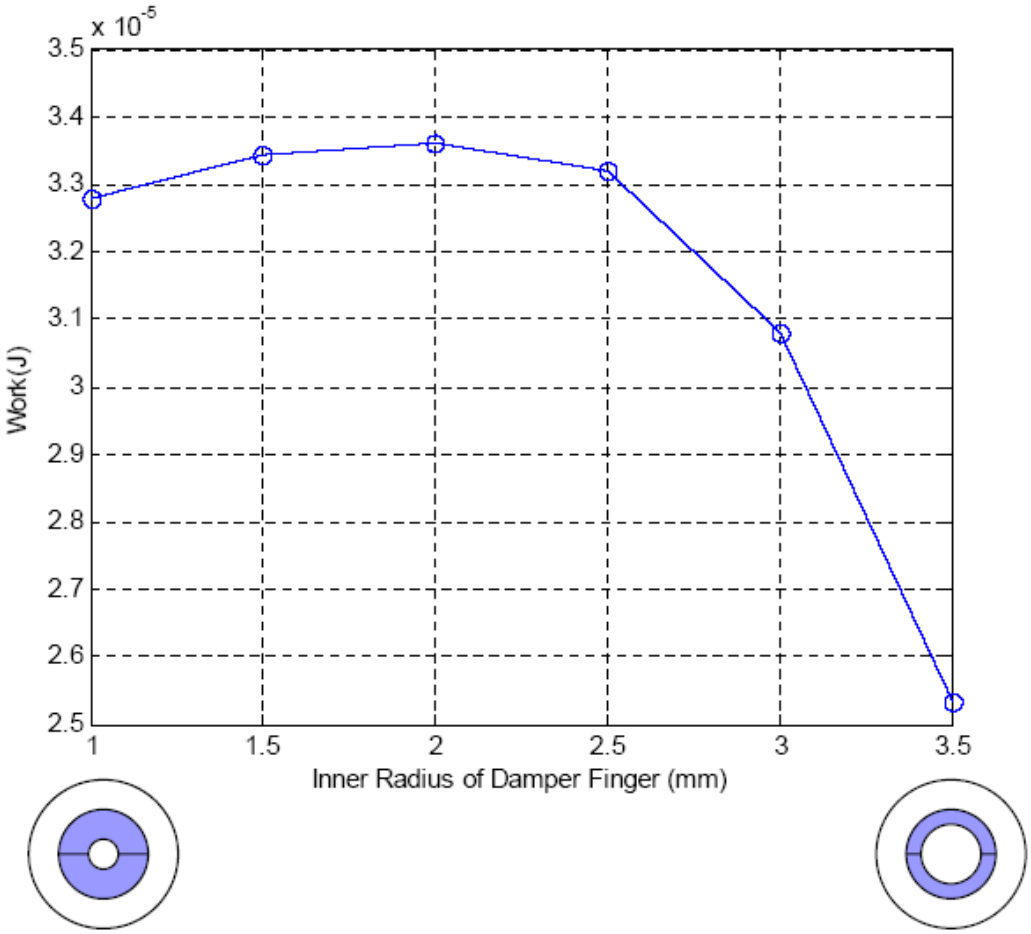

Figure 6-6: The result of the parameter study in which the inner radius of finger was changed.

Change the Number of the Finger

Next the number of fingers is changed from 2 to 10 for the case where the inner radius is 1.5 mm. The damping work shows a minimum value for the four-finger case, and a maximum value for the five-fingered case. The start angle of the finger (position of the finger) is chosen to have the maximum damping.

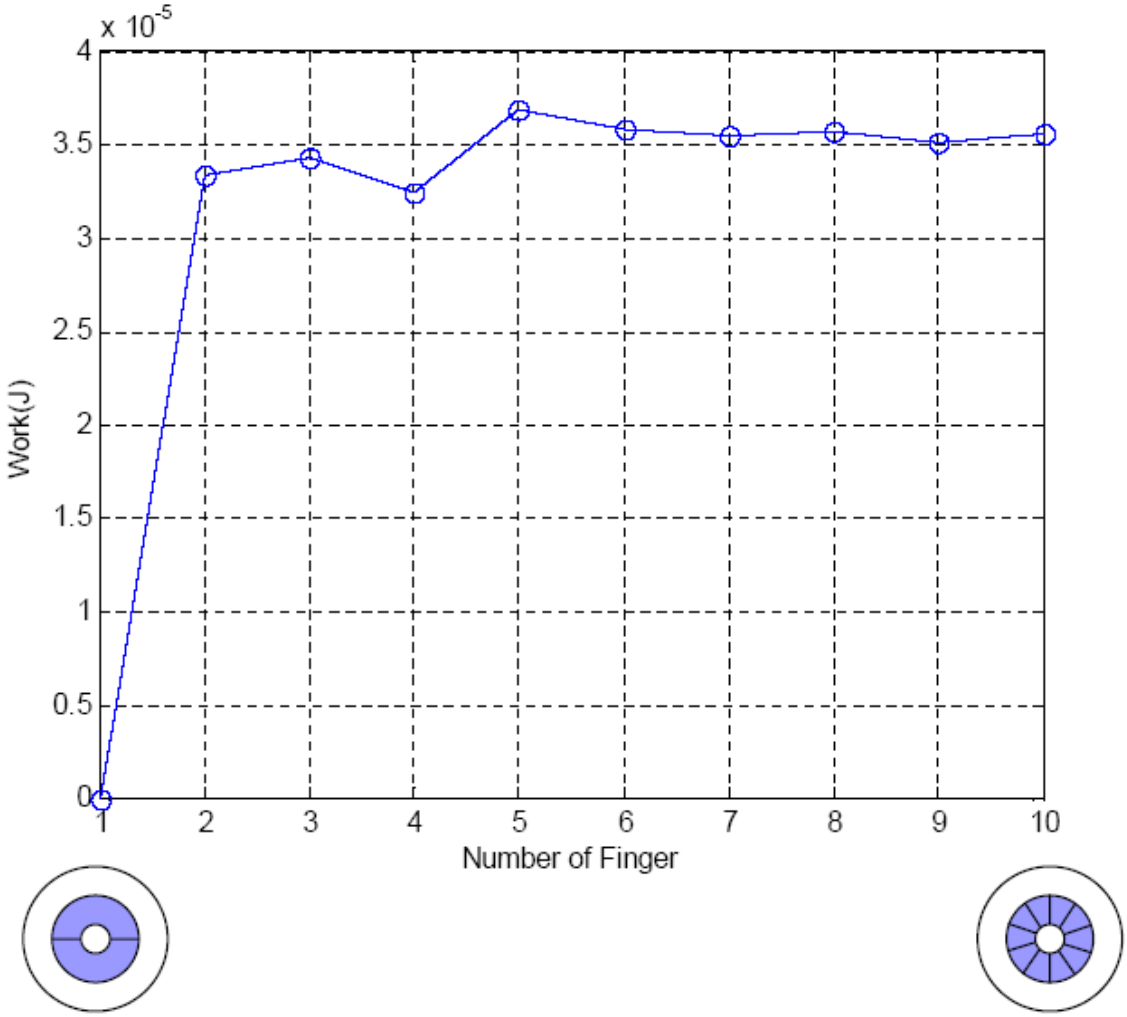

Figure 6-7. The result of the parameter study in which the number of fingers was changed.

Final Results

The parameter study is repeated for all cases, and the results are as follows.

Table 6.1: The results of parameter study									x10^{-5}J
	2	3	4	5	6	7	8	9	10
1mm	3.28	3.41	3.21	3.69	3.55	3.54	3.54	3.48	3.51
1.5mm	3.34	3.43	3.24	3.72	3.58	3.55	3.57	3.52	3.56
2.0mm	3.36	3.41	3.24	3.69	3.54	3.47	3.52	3.45	3.5
2.5mm	3.31	3.31	3.18	3.57	3.36	3.33	3.39	3.35	3.42
3.0mm	3.08	3.1	3.02	3.32	3.1	3.08	3.12	3.04	3.16
3.5mm	2.53	2.62	2.65	2.83	2.61	2.63	2.65	2.6	2.68

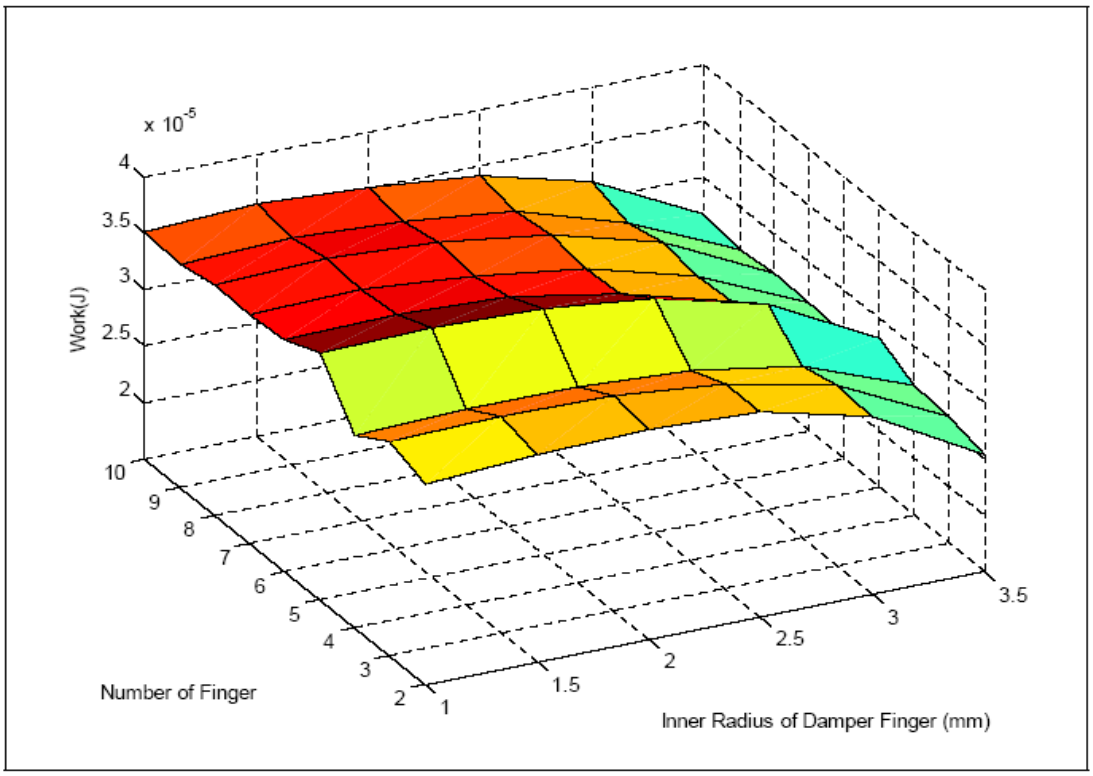

Figure 6-8: The plot of Table 6-1.

In order to find the configuration that yields the maximum damping work, the first design variable (R1) is changed by six different values and the second design variable (number of finger) is changed by nine different values. Table 6-1 shows the results in 6×9 matrix. In each configuration, the start angle is chosen such that the maximum damping work can be occurred. Figure 6-8 plots the response surface of the damping work. Even if the second design variable is discrete, a continuous surface is plotted for illustration purpose. It is noted that the local peak when the number of fingers is five is maintained throughout all different radii. The general trend of the response surface is consistent. Based on the response surface, we can conclude that the damping work has its maximum value when the inner radius is 1.5 mm and the number of fingers is 5.

As a conclusion, the effect of damping work increases as the number of fingers is increased and the inner radius is decreased.

Comparison between the Analytical and Numerical Results

Figure 6-9 shows the analytical and numerical results of friction work as a function of the number of fingers. The friction work estimated from finite element analysis is less than half of the friction work obtained from the analytical method. The possible explanations of such discrepancy are the assumption of constant contact pressure.

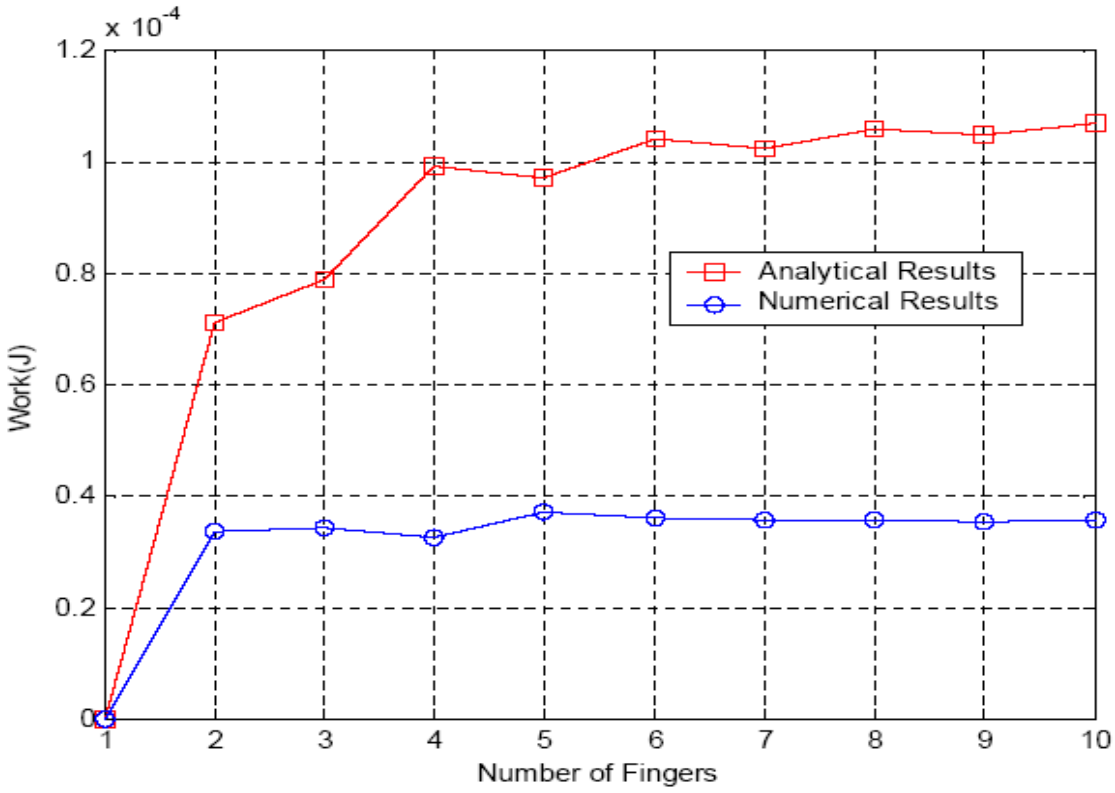

Figure 6-9: Plot of the analytical and numerical results.

In reality, the contact pressure is not constant and same portion of the finger does not contact with the shank. And most relative motion occurs at the bottom part of the end-mill. That is because the vertical force is applied at the top and the nonlinearity associated with the centrifugal force contributes the asymmetry between the top and bottom fingers. During the nonlinear analysis ANSYS automatically update the geometry and refer to the deformed configuration, which means the body force is calculated at the deformed geometry. Even

though the analytical and numerical results show the difference, the general trends of both results are very similar each other.

In order to explain the general trends of friction work, consider the analytical explanation of the contact pressure:

$$P_c = \frac{MR\,\omega^2}{A_c}$$

where $\frac{M}{A_c}$ *and* ω *are constant. Value R , which is the distance between the rotational* and the mass center of the finger, can be calculated by

$$R = \frac{2(R_2^{\,3} - R_1^{\,3})\sin\alpha}{3(R_2^{\,2} - R_1^{\,2})\alpha}$$

If we assume that the friction work is proportional to the contact pressure, then the friction work is proportional to R, which increases as the number of fingers increases. If the number of the finger increases, which means the angle α goes to zero, R converges to

$$R = \frac{2(R_2^{\,3} - R_1^{\,3})}{3(R_2^{\,2} - R_1^{\,2})}$$

Therefore, the maximum value of the contact pressure can be calculated by

$$P_c = \frac{MR\omega^2}{A_c} = \frac{2(R_2^{\,3} - R_1^{\,3})}{3(R_2^{\,2} - R_1^{\,2})}\frac{M\omega^2}{A_c}$$

As a conclusion, the friction work increases along with the number of fingers, but its effect is reduced as the number of fingers increases.

Chapter 7
Conclusion and Future Work

The goal of this research was to design the mechanical damper which is inserted into the end-mill. Through the nonlinear finite element analysis and parameter study, the trend of the damping effect is identified.

The results from the analytical method were used to verify the FEA result. Although the number and the inner radius of finger were varied in finite element analysis, only the two-finger case was considered in the comparison. The FEA results were smaller than those of the analytical approach because some regions did not contact and the contact pressure was not constant.

A parameter study was carried out by changing the inner radius and the number of fingers. The inner radius was varied from 1.0 mm to 3.5 mm, and the number of fingers was varied from 2 to 10. The results show general trends of the damping work according to the change of the two design variables. As the inner radius decreased and the number of finger increased, the damping work increased. The Maximum value was 3.27×10^{-5}J when the inner radius was 1.5 mm and the numbers of fingers were 5. The parameter study also showed that when the number of the fingers is small the damping work is affected by the position of the finger, but that this dependence disappears as the number of finger increases.

7.1 Recommendations for Future Research

As discussed in Chapter 6, the damping work depends on the start angle. However, in practice the end-mill is continuously rotating. Thus, it is recommended to perform a series of static FEA by rotating the end-mill by on cycle and to calculate the integrated damping work. This procedure will provide more accurate estimation of the real damping work.

APPENDIX

Matlab Code for Theoretical Analysis

```
%-------------------------------------------------------------------------------
% Matlab function to calculate the work done by the friction force
%
%
%-------------------------------------------------------------------------------
function cal_work
%-------------------------------------------------------------------------------
% Material Properties, radius and applied forces.
%-------------------------------------------------------------------------------
E=2.0678e11;        %- Modulus of Elasticity : 2.0*10^11[MPa]
rho=7820;           %- Mass Density : 7820[kg/m^3]
mu=0.15;            %- Friction Coefficient : 0.15
r1=1.5e-3;
r2=4.7625e-3;
r3=r2;
r4=9.525e-3;
L=101.6e-3;
omega=2722;
F=100;
%-------------------------------------------------------------------------------
% Calculate the work according to the change of the inner radius of finger.
%-------------------------------------------------------------------------------
n=2; m=1;
for r1=1.0e-3:0.5e-3:3.5e-3
  ang(1)=0;
  for i=1:n
     ang(i+1)=ang(1)+(360/n)*i;
  end
  ang=ang*(pi/180);
  II=(1/4)*((r4)^4-(r3)^4)*pi;
  for i=1:(n-1)
     tmp1=failingang(i+1))*cos(ang(i+1))-sin(ang(i))*cos(ang(i))-(ang(i+1)-ang(i));
     tmp1=tmp1*((r1)^4-(r2)^4);
     tmp1=tmp1*(1/8);
     II=II+tmp1;
  end
  work=0;
  for i=1:n
     alpha=(ang(i+1)-ang(i))/2;
      d1=(2*sin(alpha).*(r2^3-r1^3))/(3*alpha*(r2^2-r1^2));
```

```
      d2=d1*sin((ang(i)+ang(i+1))*0.5);
      V=(ang(i+1)-ang(i))*(r2^2-r1^2)*L*0.5;
      P=abs(V*rho*(omega^2)*d1/L);
      work=work+abs((1/3)*(L^3)*mu*P*F*d2/(E*II));
   end
   y1(m)=work;
   m=m+1;
end
x1=[1.0e-3:0.5e-3:3.5e-3];
plot(x1,y1,'b-o');
grid;
xlabel('Inner Radius of Damper Finger (m)');
ylabel('Work(J)');
[tmp,n]=size(x1);
clc
fprintf ('\nCalculate the work according to the change of the inner radius of finger.\n');
fprintf ('The Number of Finger=%3.0f\nStart Angle=%3.0f [Degree]\n',n,0);
for i=1:n
   fprintf('Inner Radius of Finger =%16.9e [m]\t\tWork=%16.9e [J]\n',x1(i),y1(i));
end
%--------------------------------------------------------------------------------
% Calculate the work according to the change of the start angle of finger.
%--------------------------------------------------------------------------------
n=2;m=1;r1=1.5e-3;
atmp=(360/n)/4;
for a=0:atmp:atmp*3
   ang(1)=a;
   for i=1:n
      ang(i+1)=ang(1)+(360/n)*i;
   end
   ang=ang*(pi/180);
   II=(1/4)*((r4)^4-(r3)^4)*pi;
   for i=1:(n-1)
      tmp1=sin(ang(i+1))*cos(ang(i+1))-sin(ang(i))*cos(ang(i))-(ang(i+1)-ang(i));
      tmp1=tmp1*((r1)^4-(r2)^4);
      tmp1=tmp1*(1/8);
      II=II+tmp1;
   end
   work=0;
   for i=1:n
      alpha=(ang(i+1)-ang(i))/2;
      d1=(2*sin(alpha).*(r2^3-r1^3))/(3*alpha*(r2^2-r1^2));
      d2=d1*sin((ang(i)+ang(i+1))*0.5);
      V=(ang(i+1)-ang(i))*(r2^2-r1^2)*L*0.5;
      P=abs(V*rho*(omega^2)*d1/L);
```

```
      work=work+abs((1/3)*(L^3)*mu*P*F*d2/(E*II));
  end
  y2(m)=work;
  m=m+1;
end
x2=[0:atmp:atmp*3];
figure;
plot(x2,y2,'b-o');
grid;
xlabel('Start Angle of Damper Finger (degree)');
ylabel('Work(J)');
[tmp,n]=size(x2);
fprintf('\nCalculate the work according to the chage of the start angle of finger.\n');
fprintf('Number of Finger=%5.0f\nInner Radius of the Finger=%16.9e [m]\n',2,r1);
for i=1:n
  fprintf('Start Angle =%16.9e [Degree]\t\tWork=%16.9e [J]\n',x2(i),y2(i));
end
%-------------------------------------------------------------------------------
% Calculate the work according to the change of the number of finger.
%-------------------------------------------------------------------------------
m=1;clear ang
for n=2:10
  clear ang
  atmp=(1+(-1)^(n-1))/2;
  ang(1)=((360/n)/4)*atmp;
  for i=1:n
     ang(i+1)=ang(1)+(360/n)*i;
  end
  ang=ang*(pi/180);
  II=(1/4)*((r4)^4-(r3)^4)*pi;
  for i=1:(n-1)
     tmp1=sin(ang(i+1))*cos(ang(i+1))-sin(ang(i))*cos(ang(i))-(ang(i+1)-ang(i));
     tmp1=tmp1*((r1)^4-(r2)^4);
     tmp1=tmp1*(1/8);
     II=II+tmp1;
  end
  work=0;
  for i=1:n
     alpha=(ang(i+1)-ang(i))/2;
     d1=(2*sin(alpha).*(r2^3-r1^3))/(3*alpha*(r2^2-r1^2));
     d2=d1*sin((ang(i)+ang(i+1))*0.5);
     V=(ang(i+1)-ang(i))*(r2^2-r1^2)*L*0.5;
     P=abs(V*rho*(omega^2)*d1/L);
     work=work+abs((1/3)*(L^3)*mu*P*F*d2/(E*II));
  end
```

```
   y3(m+1)=work;
    m=m+1;
end
x3=[1:10];
figure;
plot(x3,y3,'b-o');
axis([0,10,0,11e-5]);
grid;
xlabel('Number of Damper Finger');
ylabel('Work(J)');
[tmp,n]=size(x3);
fprintf('\nCalculate the work according to the change of the number of finger.\n');
fprintf('Inner Radius of the Finger=%16.9e [m]\n',r1);
for i=1:n
   fprintf('Number of Finger =%3.0f\t\tWork=%16.9e [J]\n',x3(i),y3(i));
end
```

References

1. Shigley, J.E., "Machine Design,"NY 1976.
2. Slocum,A.H., Precision Machine Design, Prentice Hall,Inc.,Englehood Cliffs, NJ, 1992.
3. Tlusty, J., Manufacturing Processes and Equipment, Prentice Hall, Inc., Upper Saddle River, NJ, 2000.
4. Sterling, Robert A., "Damping of Long Endmills,"Master's Thesis, University of Denver, 1985.
5. Zhong, Z.H., Finite Element Procedures for Contact-Impact Problems, NY, Oxford University Press, 1993.
6. Boresi, A.P., Schmidt, R.J. and Sidebottom,O.M., Advanced Mechanics of Materials, fifth edition, John Wiley and Sons, Inc., Ny,1993.